

# Minimizing Total Biharmonic Distance in Large Graphs via Link Recommendation

Xinna Zhou

College of Computer Science and Artificial Intelligence  
Fudan University  
Shanghai, China  
23210240097@m.fudan.edu.cn

Zhongzhi Zhang\*

College of Computer Science and Artificial Intelligence  
Fudan University  
Shanghai, China  
zhangzz@fudan.edu.cn

## Abstract

The total biharmonic distance, which is the sum of the biharmonic distance between every pair of nodes in a network, is a key metric for evaluating network connectivity and robustness. In this paper, we study the problem of minimizing the total biharmonic distance by adding  $k$  nonexistent edges for a given graph  $G$  and budget  $k$ . The problem is computationally challenging. We show that the objective function of the problem is monotone but not supermodular. To solve this problem, we propose simple greedy algorithms with cubic time complexity. To mitigate the high time complexity of these greedy algorithms, we apply several techniques, including the projection method, the Laplacian solver, and convex hull approximation. These techniques reduce the time complexity of our proposed algorithms from cubic to nearly linear while providing error guarantees. Finally, extensive experiments on real datasets demonstrate both the efficiency and effectiveness of our proposed algorithms.

This paper has been published in Proceedings of the 32nd ACM SIGKDD Conference on Knowledge Discovery and Data Mining V.1 (KDD '26). DOI: <https://doi.org/10.1145/3770854.3780204>.

## CCS Concepts

• **Theory of computation** → **Graph algorithms analysis**.

## Keywords

Combinatorial optimization; biharmonic distance; resistance distance; connectivity; link addition; graph algorithm

## 1 Introduction

Graph distance metrics play a crucial role in the realm of network analysis. Notable distance metrics include geodesic distance [50] and resistance distance [31]. Resistance distance originates from electrical network theory and has been widely utilized in clustering [60], graph learning [9, 33, 81], and collaborative recommendation systems [22, 35]. Additionally, it has been applied to ranking problems in large graphs [58], detecting anomalous changes in graph structure over time [64], assessing node significance [45], and enhancing the efficiency of graph systems [54]. Over the past few decades, considerable efforts have been dedicated to further understanding and exploring the properties of resistance distance [18, 19, 67].

Resistance distance has several variants [71], among which biharmonic distance [43] stands out. It was introduced to capture more

nuanced local and global structural information, offering advantages over resistance distance in many applications, such as maintaining graph connectivity and identifying critical cut edges [8]. Biharmonic distance has been applied across various domains, including graph clustering [8], graph embedding techniques [9, 33], graph matching [20], network coherence [78, 79], leader selection in noisy networks [21], identifying crucial edges [76], and other network science problems [6, 70].

Beyond individual metrics, the aggregate of a metric in a graph is often used to evaluate the overall network. For instance, the Kirchhoff index sums the resistance distances between all node pairs [25, 31]. Similarly, the total biharmonic distance, or biharmonic index [78], is the sum of biharmonic distances across all node pairs in the graph. These aggregate metrics serve as powerful tools for evaluating various properties of a network and have attracted significant attention. The Kirchhoff index is key for measuring network connectedness [68] and evaluating the robustness of consensus algorithms [53]. The total biharmonic distance can be expressed by the Kirchhoff index and the resistance distances between some node pairs [69]. The total biharmonic distance has many application scenarios. It can effectively evaluate the robustness of second-order consensus algorithms in distributed network systems [69, 73] and identify local vulnerabilities [70]. For example, in power grids and complex oscillator networks, total biharmonic distance can measure the fault tolerance of the system [70]. In communication networks, when lines are cut and information must be redirected, total biharmonic distance can evaluate a network's vulnerability to changes [69]. In addition, it is an important tool for evaluating network connectivity [8] and can also be used to define edge importance metrics [61].

Networks with smaller total biharmonic distance are known to exhibit enhanced robustness and stronger connectivity, leading to improved overall system performance [6, 78]. Therefore, optimizing total biharmonic distance through different graph operations becomes essential. Motivated by practical scenarios such as link recommendation in online social networks, we study the problem of optimizing (minimizing) total biharmonic distance by adding nonexistent edges (links) to a graph. More precisely, we aim to devise effective and efficient algorithms for the following optimization problem: For a given connected undirected unweighted graph  $G = (V, E)$  with  $n$  nodes and  $m$  edges, a small positive integer  $k$ , how to add  $k$  nonexistent edges from a candidate edge set  $Q = (V \times V) \setminus E$  to graph  $G$ , so that the total biharmonic distance for the resulting graph is minimized.

The main contributions of this paper are summarized below.

- We show that the total biharmonic distance is monotonically decreasing but not supermodular. We then propose a simple greedy

\*Corresponding author.

algorithm with cubic time complexity, providing an approximation guarantee based on the curvature and submodularity ratio of the objective function. We also present a gradient-based greedy algorithm as a novel approach to address this problem.

- We employ several techniques, including random projection, the Laplacian solver, and convex hull approximation, resulting in a scalable and efficient algorithm APPROXFAST. This algorithm is gradient-based and achieves a time complexity of  $\tilde{O}(k(nl+m)/\epsilon^2)$ , where  $\tilde{O}(\cdot)$  hides  $\text{poly}(\log(n))$  factors,  $\epsilon > 0$  is the error parameter that balances performance and efficiency, and  $l$  represents the number of nodes on the boundary of the approximate convex hull, which is typically small in most real-world networks.

- We evaluate our algorithms by performing experiments on many real-world networks of varying scales, showing that our proposed fast algorithm APPROXFAST achieves both good efficiency and effectiveness and is scalable to large networks with over four million nodes.

## 2 Preliminaries

### 2.1 Notations

We use  $\mathbb{R}$  to denote real number field. We utilize bold lowercase (e.g.,  $\mathbf{x}$ ) for vectors and uppercase (e.g.,  $\mathbf{M}$ ) for matrices. Elements are indicated by subscripts, e.g.,  $x_i$  or  $M_{i,j}$ . For a matrix  $\mathbf{M}$ ,  $\mathbf{M}[i, \cdot]$  and  $\mathbf{M}[:, j]$  represent the  $i$ -th row and  $j$ -th column, respectively. Let  $\mathbf{e}_i$  denote the  $i$ -th standard basis vector (1 at position  $i$ , 0 elsewhere). We use  $\mathbf{1}$  (resp.  $\mathbf{J}$ ) to denote the all-ones (column) vector (resp. matrix). We write  $\mathbf{x}^\top$  and  $\mathbf{M}^\top$  to represent the transposes of vector  $\mathbf{x}$  and matrix  $\mathbf{M}$ , respectively. For any vector  $\mathbf{a}$ , we use  $\|\mathbf{a}\| = \sqrt{\sum_i a_i^2}$  to denote the  $\ell_2$  norm of  $\mathbf{a}$ , and use  $\|\mathbf{a}\|_X = \sqrt{\mathbf{a}^\top \mathbf{X} \mathbf{a}}$  to denote the matrix norm of  $\mathbf{a}$  for matrix  $\mathbf{X}$ . For two non-negative scalars  $a$  and  $b$ , we use  $a \approx_\epsilon b$  to denote that  $a$  is an  $\epsilon$ -approximation of  $b$  obeying relation  $(1-\epsilon)b \leq a \leq (1+\epsilon)b$ . For two matrices  $\mathbf{A}$  and  $\mathbf{B}$ , we write  $\mathbf{A} \preceq \mathbf{B}$  to denote that  $\mathbf{B} - \mathbf{A}$  is positive semi-definite, i.e.,  $\mathbf{x}^\top \mathbf{A} \mathbf{x} \leq \mathbf{x}^\top \mathbf{B} \mathbf{x}$  holds for every vector  $\mathbf{x}$ .

### 2.2 Graph and Related Matrices

Let  $G = (V, E)$  be a connected undirected graph with  $V = \{1, 2, \dots, n\}$  and  $E = \{e_1, e_2, \dots, e_m\}$ . The adjacency matrix  $\mathbf{A} \in \{0, 1\}^{n \times n}$  satisfies  $A_{i,j} = 1$  if nodes  $i$  and  $j$  are adjacent, and 0 otherwise. The degree matrix is  $\mathbf{D} = \text{diag}(d_1, \dots, d_n)$ , where  $d_i = \sum_{j=1}^n A_{i,j}$ , and the Laplacian matrix is  $\mathbf{L} = \mathbf{D} - \mathbf{A}$ . If we fix an arbitrary orientation for all edges in  $G$ , then we define the signed edge-vertex incidence matrix  $\mathbf{B} \in \mathbb{R}^{m \times n}$ , whose entries are:  $B_{e,u} = 1$  if node  $u$  is the head of edge  $e$ ,  $B_{e,u} = -1$  if node  $u$  is the tail of edge  $e$ , and  $B_{e,u} = 0$  otherwise.  $\mathbf{L}$  can also be represented by  $\mathbf{L} = \mathbf{B}^\top \mathbf{B}$ . For any pair of distinct nodes  $u, v \in V$ , we define  $\mathbf{b}_{uv} = \mathbf{e}_u - \mathbf{e}_v$ . If an edge  $e$  connects  $u$  and  $v$  and we fix an arbitrary orientation such that  $e$  is directed from  $u$  to  $v$ , we define  $\mathbf{b}_e = \mathbf{e}_u - \mathbf{e}_v$ . Since  $\mathbf{L}$  is symmetric, it has eigenvalues  $0 = \lambda_1(\mathbf{L}) < \lambda_2(\mathbf{L}) \leq \dots \leq \lambda_n(\mathbf{L})$  with corresponding orthonormal eigenvectors  $\mathbf{u}_1, \mathbf{u}_2, \dots, \mathbf{u}_n$ , and can be written as  $\mathbf{L} = \sum_{i=2}^n \lambda_i \mathbf{u}_i \mathbf{u}_i^\top$ . Its Moore-Penrose pseudoinverse is  $\mathbf{L}^\dagger = (\mathbf{L} + \frac{1}{n} \mathbf{J})^{-1} - \frac{1}{n} \mathbf{J}$ . We have  $\frac{1}{2n^4} \mathbf{L} \mathbf{L}^\dagger \preceq \mathbf{L} \preceq n \mathbf{I}$  and  $\frac{1}{n} \mathbf{L} \mathbf{L}^\dagger \preceq \mathbf{L}^\dagger \preceq 2n^4 \mathbf{I}$  [12]. The eigenvalues and the corresponding eigenvectors of  $\mathbf{L}^2$  are  $\lambda_i^2$  and  $\mathbf{u}_i$ ,  $i = 1, 2, \dots, n$ . Thus,  $\mathbf{L}^2$  has the following spectral decomposition:  $\mathbf{L}^2 = \sum_{i=2}^n \lambda_i^2(\mathbf{L}) \mathbf{u}_i \mathbf{u}_i^\top$ ,

which indicates that  $\mathbf{L}^2$  is positive semi-definite with only one zero eigenvalue. Its Moore-Penrose pseudo-inverse  $\mathbf{L}^{2\dagger}$  is positive semi-definite with only one zero eigenvalue. Similarly,  $\mathbf{L}^3$  and  $\mathbf{L}^{3\dagger}$  are positive semi-definite with only one zero eigenvalue. For any edge set  $T \subseteq (V \times V) \setminus E$ , let  $G_T = (V, E \cup T)$  be the graph after adding edges in  $T$ .

### 2.3 Biharmonic Distances and Related Metrics

DEFINITION 2.1 ([76]). For a graph  $G = (V, E)$ , the biharmonic distance  $\mathbf{b}(u, v)$  between any pair of distinct nodes  $u, v$  is defined by

$$\mathbf{b}(u, v) = \sqrt{\mathbf{b}_{uv}^\top \mathbf{L}^{2\dagger} \mathbf{b}_{uv}} = \|\mathbf{L}^\dagger \mathbf{b}_{uv}\| = \sqrt{\mathbf{L}_{u,u}^{2\dagger} + \mathbf{L}_{v,v}^{2\dagger} - 2\mathbf{L}_{u,v}^{2\dagger}}.$$

We denote the square of the biharmonic distance as  $\mathbf{b}^2(u, v)$ . For brevity, we will sometimes refer to  $\mathbf{b}^2(u, v)$  as the biharmonic distance, when the context makes it clear that we mean its square. Based on the biharmonic distance, we can derive the following graph index.

DEFINITION 2.2 ([77]). For a graph  $G = (V, E)$ , the total biharmonic distance  $B(G)$  is defined by

$$B(G) = \frac{1}{2} \sum_{u \in V} \sum_{v \in V} \mathbf{b}^2(u, v) = n \sum_{i=2}^n \frac{1}{\lambda_i^2} = n \text{Tr}(\mathbf{L}^{2\dagger}).$$

The biharmonic distance can be further generalized to higher-order variants [61] by considering arbitrary powers of  $\mathbf{L}^\dagger$ .

DEFINITION 2.3 ([8]). For a graph  $G = (V, E)$ , the  $k$ -harmonic distance  $\mathbf{h}_k(u, v)$  between any pair of distinct nodes  $u, v$  is defined by

$$\mathbf{h}_k(u, v) = \sqrt{\mathbf{b}_{uv}^\top \mathbf{L}^{k\dagger} \mathbf{b}_{uv}}.$$

Similarly, we will refer to  $\mathbf{h}_k^2(u, v)$  as the  $k$ -harmonic distance, rather than the square of the  $k$ -harmonic distance, when the context is clear. Notably, when  $k = 1$ ,  $\mathbf{h}_k^2(u, v) = R_{uv}$  which is the resistance distance between nodes  $u$  and  $v$ . When  $k = 2$ ,  $\mathbf{h}_k(u, v) = \mathbf{b}(u, v)$  which is the biharmonic distance between nodes  $u$  and  $v$ . We also introduce the total  $k$ -harmonic distance.

DEFINITION 2.4 ([70]). For a graph  $G = (V, E)$ , the total  $k$ -harmonic distance  $K(G)$  is defined by

$$K(G) = \frac{1}{2} \sum_{u \in V} \sum_{v \in V} \mathbf{h}_k^2(u, v) = n \sum_{i=2}^n \frac{1}{\lambda_i^k} = n \text{Tr}(\mathbf{L}^{k\dagger}).$$

## 3 Problem Formulation

In this section, we begin by examining the monotonicity of the total biharmonic distance. Next, we present the problem statement. We then analyze the properties of the objective function before introducing two simple greedy algorithms.

### 3.1 Monotonicity of Total Biharmonic Distance

The monotonically decreasing property of the total biharmonic distance was shown in [72]. However, the method in [72] does not give the marginal decrease, which is important for our algorithm. We take a different approach by first deriving the marginal decrease in total biharmonic distance when an edge is added.

LEMMA 3.1. For a connected graph  $G = (V, E)$ , the marginal decrease of the total biharmonic distance after adding an edge  $e$  is

$$\Delta(e) = B(G) - B(G_{\{e\}}) = -n \frac{(\mathbf{b}_e^\top \mathbf{L}^{2\ddagger} \mathbf{b}_e)^2}{(1 + \mathbf{b}_e^\top \mathbf{L}^\ddagger \mathbf{b}_e)^2} + n \frac{2\mathbf{b}_e^\top \mathbf{L}^{3\ddagger} \mathbf{b}_e}{1 + \mathbf{b}_e^\top \mathbf{L}^\ddagger \mathbf{b}_e}.$$

**Proof.** By Definition 2.2,  $\Delta(e) = n\text{Tr}(\mathbf{L}^{2\ddagger}) - n\text{Tr}((\mathbf{L} + \mathbf{b}_e \mathbf{b}_e^\top)^{2\ddagger})$ . Using the Sherman-Morrison formula [47], we have

$$(\mathbf{L} + \mathbf{b}_e \mathbf{b}_e^\top)^\ddagger = \mathbf{L}^\ddagger - \frac{\mathbf{L}^\ddagger \mathbf{b}_e \mathbf{b}_e^\top \mathbf{L}^\ddagger}{1 + \mathbf{b}_e^\top \mathbf{L}^\ddagger \mathbf{b}_e}. \quad (1)$$

Squaring both sides, we obtain

$$\begin{aligned} (\mathbf{L} + \mathbf{b}_e \mathbf{b}_e^\top)^{2\ddagger} &= \left( \mathbf{L}^\ddagger - \frac{\mathbf{L}^\ddagger \mathbf{b}_e \mathbf{b}_e^\top \mathbf{L}^\ddagger}{1 + \mathbf{b}_e^\top \mathbf{L}^\ddagger \mathbf{b}_e} \right)^2 \\ &= \mathbf{L}^{2\ddagger} - \frac{\mathbf{L}^{2\ddagger} \mathbf{b}_e \mathbf{b}_e^\top \mathbf{L}^\ddagger}{1 + \mathbf{b}_e^\top \mathbf{L}^\ddagger \mathbf{b}_e} - \frac{\mathbf{L}^\ddagger \mathbf{b}_e \mathbf{b}_e^\top \mathbf{L}^{2\ddagger}}{1 + \mathbf{b}_e^\top \mathbf{L}^\ddagger \mathbf{b}_e} + \frac{(\mathbf{L}^\ddagger \mathbf{b}_e \mathbf{b}_e^\top \mathbf{L}^\ddagger)^2}{(1 + \mathbf{b}_e^\top \mathbf{L}^\ddagger \mathbf{b}_e)^2}. \end{aligned} \quad (2)$$

Thus, we have

$$\begin{aligned} \text{Tr}((\mathbf{L} + \mathbf{b}_e \mathbf{b}_e^\top)^{2\ddagger}) &= \text{Tr}(\mathbf{L}^{2\ddagger}) - \frac{2\text{Tr}(\mathbf{L}^{2\ddagger} \mathbf{b}_e \mathbf{b}_e^\top \mathbf{L}^\ddagger)}{1 + \mathbf{b}_e^\top \mathbf{L}^\ddagger \mathbf{b}_e} \\ &\quad + \frac{\text{Tr}(\mathbf{L}^\ddagger \mathbf{b}_e \mathbf{b}_e^\top \mathbf{L}^{2\ddagger} \mathbf{b}_e \mathbf{b}_e^\top \mathbf{L}^\ddagger)}{(1 + \mathbf{b}_e^\top \mathbf{L}^\ddagger \mathbf{b}_e)^2}. \end{aligned}$$

Therefore, one can conclude that

$$\begin{aligned} \Delta(e) &= -n \frac{\text{Tr}(\mathbf{L}^\ddagger \mathbf{b}_e \mathbf{b}_e^\top \mathbf{L}^{2\ddagger} \mathbf{b}_e \mathbf{b}_e^\top \mathbf{L}^\ddagger)}{(1 + \mathbf{b}_e^\top \mathbf{L}^\ddagger \mathbf{b}_e)^2} + n \frac{2\text{Tr}(\mathbf{L}^{2\ddagger} \mathbf{b}_e \mathbf{b}_e^\top \mathbf{L}^\ddagger)}{1 + \mathbf{b}_e^\top \mathbf{L}^\ddagger \mathbf{b}_e} \\ &= -n \frac{\mathbf{b}_e^\top \mathbf{L}^{2\ddagger} \mathbf{b}_e \text{Tr}(\mathbf{L}^\ddagger \mathbf{b}_e \mathbf{b}_e^\top \mathbf{L}^\ddagger)}{(1 + \mathbf{b}_e^\top \mathbf{L}^\ddagger \mathbf{b}_e)^2} + n \frac{2\text{Tr}(\mathbf{b}_e^\top \mathbf{L}^{3\ddagger} \mathbf{b}_e)}{1 + \mathbf{b}_e^\top \mathbf{L}^\ddagger \mathbf{b}_e} \\ &= -n \frac{(\mathbf{b}_e^\top \mathbf{L}^{2\ddagger} \mathbf{b}_e)^2}{(1 + \mathbf{b}_e^\top \mathbf{L}^\ddagger \mathbf{b}_e)^2} + n \frac{2\mathbf{b}_e^\top \mathbf{L}^{3\ddagger} \mathbf{b}_e}{1 + \mathbf{b}_e^\top \mathbf{L}^\ddagger \mathbf{b}_e}. \end{aligned} \quad (3)$$

This finishes the proof.  $\square$

Building on Lemma 3.1, we now prove the monotonicity of total biharmonic distance in Lemma 3.2.

LEMMA 3.2. Let  $G = (V, E)$  be a connected graph with  $n$  nodes and  $e \in (V \times V) \setminus E$ . Then  $B(G_{\{e\}}) < B(G)$ , that is,  $B(G)$  is monotonically decreasing.

**Proof.** Suppose  $\mathbf{u} = \mathbf{B}\mathbf{L}^{2\ddagger} \mathbf{b}_e$ ,  $\mathbf{v} = \mathbf{B}\mathbf{L}^\ddagger \mathbf{b}_e$ , thus

$$\mathbf{u}^\top \mathbf{u} = \mathbf{b}_e^\top \mathbf{L}^{2\ddagger} \mathbf{B}^\top \mathbf{B} \mathbf{L}^{2\ddagger} \mathbf{b}_e = \mathbf{b}_e^\top \mathbf{L}^{2\ddagger} \mathbf{L} \mathbf{L}^{2\ddagger} \mathbf{b}_e = \mathbf{b}_e^\top \mathbf{L}^{3\ddagger} \mathbf{b}_e.$$

Likewise,  $\mathbf{v}^\top \mathbf{v} = \mathbf{b}_e^\top \mathbf{L}^\ddagger \mathbf{b}_e$ ,  $\mathbf{u}^\top \mathbf{v} = \mathbf{b}_e^\top \mathbf{L}^{2\ddagger} \mathbf{b}_e$ . By Cauchy-Schwarz inequality [65], we have  $(\mathbf{u}^\top \mathbf{v})^2 \leq (\mathbf{u}^\top \mathbf{u})(\mathbf{v}^\top \mathbf{v})$ , implying

$$(\mathbf{b}_e^\top \mathbf{L}^{2\ddagger} \mathbf{b}_e)^2 \leq \mathbf{b}_e^\top \mathbf{L}^{3\ddagger} \mathbf{b}_e \mathbf{b}_e^\top \mathbf{L}^\ddagger \mathbf{b}_e.$$

According to Lemma 3.1, we have

$$\begin{aligned} \Delta(e) &\geq -n \frac{\mathbf{b}_e^\top \mathbf{L}^{3\ddagger} \mathbf{b}_e \mathbf{b}_e^\top \mathbf{L}^\ddagger \mathbf{b}_e}{(1 + \mathbf{b}_e^\top \mathbf{L}^\ddagger \mathbf{b}_e)^2} + n \frac{2\mathbf{b}_e^\top \mathbf{L}^{3\ddagger} \mathbf{b}_e (1 + \mathbf{b}_e^\top \mathbf{L}^\ddagger \mathbf{b}_e)}{(1 + \mathbf{b}_e^\top \mathbf{L}^\ddagger \mathbf{b}_e)^2} \\ &= n \frac{2\mathbf{b}_e^\top \mathbf{L}^{3\ddagger} \mathbf{b}_e + \mathbf{b}_e^\top \mathbf{L}^{3\ddagger} \mathbf{b}_e \mathbf{b}_e^\top \mathbf{L}^\ddagger \mathbf{b}_e}{(1 + \mathbf{b}_e^\top \mathbf{L}^\ddagger \mathbf{b}_e)^2} > 0. \end{aligned}$$

This establishes that  $\Delta(e) > 0$ , thereby completing the proof.  $\square$

This lemma indicates that adding any nonexistent edge to  $G$  decreases the total biharmonic distance. Since a smaller biharmonic distance indicates better performance, it is useful in applications like assessing the robustness of second-order consensus algorithms in noisy networks [6, 78]. This motivates our exploration of minimizing the total biharmonic distance by adding  $k$  new edges.

## 3.2 Problem Statement

We now give a mathematical formulation of our problem.

PROBLEM 1. Given a connected graph  $G = (V, E)$ , a candidate edge set  $Q = (V \times V) \setminus E$  and an integer  $k \leq |Q|$ , find a subset  $T \subseteq Q$  of  $k$  edges such that the total biharmonic distance of the graph  $G^* = (V, E \cup T^*)$  is minimized. More formally, the objective is to find

$$T^* = \arg \min_{T \subseteq Q, |T|=k} B(G_T).$$

Problem 1 is inherently a combinatorial problem, which is computationally challenging.

## 3.3 Properties of Objective Function

We have already proved that the objective function of Problem 1  $B(\cdot)$  is monotone in Lemma 3.2. Next, we show that function  $B(\cdot)$  is not supermodular.

LEMMA 3.3. The objective function in Problem 1, specifically the total biharmonic distance  $B(\cdot)$ , is not supermodular. This means that there exist two edge sets  $S$  and  $T$  such that  $S \subset T \subseteq Q$ , and an edge  $e \in Q \setminus T$ , for which the following inequality holds

$$B(G_{S \cup \{e\}}) - B(G_S) > B(G_{T \cup \{e\}}) - B(G_T).$$

**Proof.** To prove the non-supermodularity of the objective function, consider the graph shown in Figure 1. The solid black lines denote the edges of the original graph, the solid blue line represents the edge in  $T$ , and the dashed red line indicates the edge  $e$ . We define  $S = \emptyset$ ,  $T = \{(1, 3)\}$ , and  $e = (1, 4)$ . The computation yields  $B(G_{S \cup \{e\}}) - B(G_S) = -0.89$  and  $B(G_{T \cup \{e\}}) - B(G_T) = -1.01$ , violating the condition of supermodularity since  $-0.89 > -1.01$ . Therefore, the objective function is non-supermodular.  $\square$

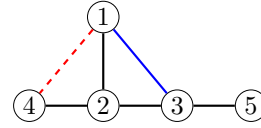


Figure 1: A counterexample with 5 nodes for Lemma 3.3.

For traditional monotonically decreasing and supermodular functions, a simple greedy strategy can attain an approximation ratio of  $(1 - 1/e)$  solution in each iteration [49]. Despite the objective function  $B(\cdot)$  being not supermodular, the greedy method can still remain a suitable strategy for solving Problem 1 with guaranteed performance. We define the non-negative, monotone-increasing function  $f(T) = B(G) - B(G_T)$ , where  $T \subseteq Q$ . We introduce a new quantity  $\Theta_T(S) = f(S \cup T) - f(S)$ , which represents the marginal benefit of adding the set  $T \subseteq Q$  to the set  $S \subseteq Q$ . Utilizing this, we introduce the concepts of submodularity ratio and curvature.

DEFINITION 3.4 ([7]). For a non-negative set function  $f$ , the submodularity ratio is defined as the largest scalar  $\gamma$  such that for any two arbitrary sets  $S \subseteq Q$  and  $T \subseteq Q$ ,

$$\sum_{i \in T \setminus S} \Theta_i(S) \geq \gamma \Theta_T(S) \cdot \Omega(n^2)$$

DEFINITION 3.5 ([7]). For a non-negative set function  $f$ , the curvature is defined as the smallest scalar  $\alpha$  such that for any two arbitrary sets  $S \subseteq Q$  and  $T \subseteq Q$ , and any element  $j \in S \setminus T$ ,

$$\Theta_j(S \cup T \setminus j) \geq (1 - \alpha)\Theta_j(S \setminus j).$$

We then establish the bounds for the submodularity ratio  $\gamma$  and curvature  $\alpha$  of the function  $f(T) = B(G) - B(G_T)$ , which will be used in the next section.

LEMMA 3.6. The submodularity ratio  $\gamma$  of the function  $f(T) = B(G) - B(G_T)$ ,  $T \subseteq Q$  is bounded by  $1 > \gamma \geq \left(\frac{\lambda_2(\mathbf{L})}{n}\right)^5$ , and its curvature  $\alpha$  is constrained by  $0 < \alpha \leq 1 - \left(\frac{\lambda_2(\mathbf{L})}{n}\right)^5$ .

**Proof.** Let  $Q = (V \times V) \setminus E$  be the candidate edge set,  $S$  and  $T$  be two arbitrary subsets of  $E$ , and  $u, v$  be any two subsets of the candidate edge set  $Q$ . To begin with, we first derive a lower and upper bound for the marginal benefit function  $\Theta_T(S) = f(S \cup T) - f(S)$ , respectively. We use  $\mathbf{L}(S)$  to denote the Laplacian matrix of the resultant graph  $G_S$ . On the one hand,

$$\begin{aligned} \Theta_T(S) &= f(S \cup T) - f(S) = B(G_S) - B(G_{S \cup T}) \\ &= n\text{Tr}(\mathbf{L}(S)^{2\dagger}) - n\text{Tr}(\mathbf{L}(S \cup T)^{2\dagger}) \\ &= \sum_{i=2}^n \frac{n}{\lambda_i^2(\mathbf{L}(S))} - \frac{n}{\lambda_i^2(\mathbf{L}(S \cup T))} \\ &= n \sum_{i=2}^n \frac{(\lambda_i(\mathbf{L}(S \cup T)) - \lambda_i(\mathbf{L}(S)))(\lambda_i(\mathbf{L}(S \cup T)) + \lambda_i(\mathbf{L}(S)))}{\lambda_i^2(\mathbf{L}(S))\lambda_i^2(\mathbf{L}(S \cup T))} \\ &\geq n \frac{(\text{Tr}(\mathbf{L}(S \cup T)) - \text{Tr}(\mathbf{L}(S)))(\lambda_2(\mathbf{L}(S \cup T)) + \lambda_2(\mathbf{L}(S)))}{\lambda_n^2(\mathbf{L}(S))\lambda_n^2(\mathbf{L}(S \cup T))} \\ &= \frac{2n|T \setminus S|(\lambda_2(\mathbf{L}(S \cup T)) + \lambda_2(\mathbf{L}(S)))}{\lambda_n^2(\mathbf{L}(S))\lambda_n^2(\mathbf{L}(S \cup T))}. \end{aligned}$$

On the other hand,

$$\begin{aligned} \Theta_T(S) &= n \sum_{i=2}^n \frac{(\lambda_i(\mathbf{L}(S \cup T)) - \lambda_i(\mathbf{L}(S)))(\lambda_i(\mathbf{L}(S \cup T)) + \lambda_i(\mathbf{L}(S)))}{\lambda_i^2(\mathbf{L}(S))\lambda_i^2(\mathbf{L}(S \cup T))} \\ &\leq n \frac{(\text{Tr}(\mathbf{L}(S \cup T)) - \text{Tr}(\mathbf{L}(S)))(\lambda_n(\mathbf{L}(S \cup T)) + \lambda_n(\mathbf{L}(S)))}{\lambda_2^2(\mathbf{L}(S))\lambda_2^2(\mathbf{L}(S \cup T))} \\ &= \frac{2n|T \setminus S|(\lambda_n(\mathbf{L}(S \cup T)) + \lambda_n(\mathbf{L}(S)))}{\lambda_2^2(\mathbf{L}(S))\lambda_2^2(\mathbf{L}(S \cup T))}. \end{aligned}$$

Then, we put the above two bounds together and derive the lower bound of the submodular ratio  $\gamma$ .

$$\begin{aligned} &\frac{\sum_{e \in T \setminus S} \Theta_e(S)}{\Theta_T(S)} \\ &\geq \sum_{e \in T \setminus S} \frac{(\lambda_2(\mathbf{L}(S \cup e)) + \lambda_2(\mathbf{L}(S)))}{\lambda_n^2(\mathbf{L}(S))\lambda_n^2(\mathbf{L}(S \cup e))} \cdot \frac{\lambda_2^2(\mathbf{L}(S))\lambda_2^2(\mathbf{L}(S \cup T))}{(\lambda_n(\mathbf{L}(S \cup T)) + \lambda_n(\mathbf{L}(S)))} \\ &\geq \left(\frac{\lambda_2(\mathbf{L})}{\lambda_n(\mathbf{L}(Q))}\right)^5 = \left(\frac{\lambda_2(\mathbf{L})}{n}\right)^5. \end{aligned}$$

The last equality holds since the largest eigenvalue of the Laplacian matrix of a complete graph with  $n$  nodes is  $n$ . Similarly, we derive the upper bound of the curvature  $\alpha$ . Let  $j$  be any candidate edge in

$S \setminus T$ . Then, we have

$$\begin{aligned} &\frac{\Theta_j(S \cup T \setminus j)}{\Theta_j(S \setminus j)} \\ &\geq \frac{2n(\lambda_2(\mathbf{L}(S \cup T \setminus j)) + \lambda_2(\mathbf{L}(S \cup T)))}{\lambda_n^2(\mathbf{L}(S \cup T \setminus j))\lambda_n^2(\mathbf{L}(S \cup T))} \cdot \frac{\lambda_2^2(\mathbf{L}(S \setminus j))\lambda_2^2(\mathbf{L}(S))}{2n(\lambda_n(\mathbf{L}(S \setminus j)) + \lambda_n(\mathbf{L}(S)))} \\ &\geq \left(\frac{\lambda_2(\mathbf{L})}{\lambda_n(\mathbf{L}(Q))}\right)^5 = \left(\frac{\lambda_2(\mathbf{L})}{n}\right)^5, \end{aligned}$$

which combining with Definition 3.5 completes the proof.  $\square$

### 3.4 Simple Greedy Approach

We can solve Problem 1 by the following naïve brute-force approach. For each subset of edges  $T$  of the  $\binom{Q}{k}$  possible subsets of edges, we can compute the total biharmonic distance for its associated graph when all edges in this set are added. Then, output the subset  $T^*$  of edges, whose addition leads to the largest decrease in the total biharmonic distance. Although this method is simple, it is computationally impossible even for small networks since computing the total biharmonic distance involves inverting a matrix, a process that requires  $\Omega(n^3)$  time. This results in a total complexity of  $\Omega(\binom{Q}{k}n^3)$ , which is very expensive even for small values of  $k$ .

To address the exponential complexity, we employ greedy heuristics. Based on Lemma 3.1, we can devise a simple greedy approach choosing the largest marginal decrease in each iteration, as formulated in Algorithm 1.

---

#### Algorithm 1: DETERDIFF( $G, k$ )

---

**Input** : Graph  $G = (V, E)$ ; an integer  $k$   
**Output** : An edge set  $T \subseteq Q$  of size  $k$

- 1 Compute  $\mathbf{L}^\dagger, \mathbf{L}^{2\dagger}, \mathbf{L}^{3\dagger}$
- 2  $T = \emptyset, Q = (V \times V) \setminus E$
- 3 **for**  $i = 1$  **to**  $k$  **do**
- 4     Compute  $\Delta(e) = B(G) - B(G_{\{e\}})$  for each  $e \in Q$
- 5     Select  $e_i$  s.t.  $e_i \leftarrow \arg \max_{e \in Q} \Delta(e)$
- 6      $T \leftarrow T \cup \{e_i\}, G \leftarrow G(V, E \cup \{e_i\}), Q \leftarrow Q \setminus \{e_i\}$
- 7     Update  $\mathbf{L}^\dagger$  by (1),  $\mathbf{L}^{2\dagger}$  by (2), and  $\mathbf{L}^{3\dagger}$  by (4)
- 8 **return**  $T$

---

We maintain three matrices:  $\mathbf{L}^\dagger, \mathbf{L}^{2\dagger}$ , and  $\mathbf{L}^{3\dagger}$ . These matrices are precomputed with a time complexity of  $O(n^3)$  (Line 1). In each iteration, calculating  $\Delta(e)$  for any edge now takes  $O(1)$  per edge. Since  $\Delta(e)$  needs to be evaluated for all edges in  $Q$  to find the one with the maximum marginal decrease, the total cost per iteration is  $\Omega(n^2)$ . Upon selecting and adding an edge  $e$  to the graph,  $\mathbf{L}^\dagger, \mathbf{L}^{2\dagger}$ , and  $\mathbf{L}^{3\dagger}$  are updated using the Sherman-Morrison formula, taking  $O(n^2)$  for each update rather than directly inverting a matrix in time  $O(n^3)$ . Specifically,  $\mathbf{L}^\dagger$  is updated using (1),  $\mathbf{L}^{2\dagger}$  is updated using (2), while  $\mathbf{L}^{3\dagger}$  is updated according to the following equation:

$$\begin{aligned} (\mathbf{L} + \mathbf{b}_e \mathbf{b}_e^\top)^{3\dagger} &= \mathbf{L}^{3\dagger} + \frac{3\mathbf{L}^{2\dagger} \mathbf{b}_e \mathbf{b}_e^\top \mathbf{L}^{2\dagger} \mathbf{b}_e \mathbf{b}_e^\top \mathbf{L}^\dagger}{(1 + \mathbf{b}_e^\top \mathbf{L}^\dagger \mathbf{b}_e)^2} - \frac{3\mathbf{L}^{2\dagger} \mathbf{b}_e \mathbf{b}_e^\top \mathbf{L}^{2\dagger}}{1 + \mathbf{b}_e^\top \mathbf{L}^\dagger \mathbf{b}_e} \\ &\quad - \frac{\mathbf{L}^\dagger \mathbf{b}_e \mathbf{b}_e^\top \mathbf{L}^{2\dagger} \mathbf{b}_e \mathbf{b}_e^\top \mathbf{L}^{2\dagger} \mathbf{b}_e \mathbf{b}_e^\top \mathbf{L}^\dagger}{(1 + \mathbf{b}_e^\top \mathbf{L}^\dagger \mathbf{b}_e)^3}. \end{aligned} \quad (4)$$

Thus, Algorithm 1 has a time complexity of  $O(n^3 + kn^2)$ , much faster than the brute-force algorithm. We then analyze its approximation guarantee using the following theorem.

**THEOREM 3.7** ([7]). *The greedy algorithm offers an approximation ratio of at least  $\frac{1}{\alpha} (1 - e^{-\alpha\gamma})$  for the problem of maximizing a non-negative increasing set function  $f$  with submodularity ratio  $\gamma$  and curvature  $\alpha$ .*

Theorem 3.7, together with the bounds for the submodularity ratio  $\gamma$  and curvature  $\alpha$  of the function  $f(T) = B(G) - B(G_T)$  stated in Lemma 3.6, leads to a performance analysis for Algorithm 1. To enhance the theoretical accuracy of Algorithm 1, a larger value of  $(1 - e^{-\gamma\alpha})/\alpha$  is desirable, which can be achieved with a higher  $\gamma$  and a lower  $\alpha$ . According to Lemma 3.6, the bounds for  $\gamma$  and  $\alpha$  are closely related to  $\lambda_2(L)$ . A larger  $\lambda_2(L)$  results in a tighter theoretical bound. Since the complete graph has  $\lambda_2(L) = n$ , denser graphs are likely to yield a better approximation ratio. While the theoretical bound implies that the approximation relies heavily on the graph's structure, Algorithm 1 often performs very close to the optimal solutions in practice, as shown in Section 5.

### 3.5 Gradient-Based Greedy Approach

Traditional heuristic greedy algorithms select edges based on the maximum marginal decrease or gain in the objective function. While this approach is commonly employed, researchers have also explored using gradients or partial derivatives of the relevant function to assess the impact of edge modifications [9, 39]. In this subsection, we explore the gradient of the total biharmonic distance to characterize the significance of an edge instead of the marginal decrease  $\Delta(e)$ .

**LEMMA 3.8.** *For a connected graph  $G = (V, E)$ , the gradient of total biharmonic distance  $c(e)$  for an edge  $e \in (V \times V) \setminus E$  is  $2nb_e^\top L^{3\ddagger} b_e$ .*

**Proof.** Let  $w_e$  denote the weight of edge  $e$ . We have

$$\begin{aligned} c(e) &= \frac{\partial B(G_{\{e\}})}{\partial w_e} = n \frac{\partial \text{Tr}((L + b_e b_e^\top)^{2\ddagger})}{\partial w_e} \\ &= n \lim_{\epsilon \rightarrow 0} \frac{1}{\epsilon} \left[ \text{Tr}((L + \epsilon b_e b_e^\top)^{2\ddagger}) - \text{Tr}(L^{2\ddagger}) \right]. \end{aligned}$$

By (2), we obtain

$$\begin{aligned} &\text{Tr}((L + \epsilon b_e b_e^\top)^{2\ddagger}) - \text{Tr}(L^{2\ddagger}) \\ &= \epsilon \text{Tr} \left( \frac{L^{2\ddagger} b_e b_e^\top L^{2\ddagger}}{1 + \epsilon b_e^\top L^{2\ddagger} b_e} \right) + \epsilon \text{Tr} \left( \frac{L^\ddagger b_e b_e^\top L^\ddagger}{1 + \epsilon b_e^\top L^\ddagger b_e} \right) - \text{Tr} \left( \frac{(\epsilon L^\ddagger b_e b_e^\top L^\ddagger)^2}{(1 + \epsilon b_e^\top L^\ddagger b_e)^2} \right) \\ &= \frac{2\epsilon b_e^\top L^{3\ddagger} b_e}{1 + \epsilon b_e^\top L^{3\ddagger} b_e} - \frac{(\epsilon b_e^\top L^\ddagger b_e)^2}{(1 + \epsilon b_e^\top L^\ddagger b_e)^2}. \end{aligned}$$

Then, we can derive that

$$c(e) = n \lim_{\epsilon \rightarrow 0} \frac{1}{\epsilon} \left[ \frac{2\epsilon b_e^\top L^{3\ddagger} b_e}{1 + \epsilon b_e^\top L^{3\ddagger} b_e} - \frac{(\epsilon b_e^\top L^\ddagger b_e)^2}{(1 + \epsilon b_e^\top L^\ddagger b_e)^2} \right] = 2nb_e^\top L^{3\ddagger} b_e.$$

This completes the proof.  $\square$

For each edge  $e \in (V \times V) \setminus E$ , the gradient of the total biharmonic distance is given by  $2nb_e^\top L^{3\ddagger} b_e$ . Since  $n$  is constant, the critical term reduces to  $b_e^\top L^{3\ddagger} b_e$ . We redefine  $c(e)$  as  $b_e^\top L^{3\ddagger} b_e$ . This leads to a gradient-based greedy algorithm that iteratively selects the edge with the largest gradient, as described in Algorithm 2. The time

complexity of this algorithm is  $O(n^3 + kn^2)$ , following a similar analysis to that of Algorithm 1. One interesting finding is that  $c(e)$  is exactly the 3-harmonic distance. Recalling that the gradient of the Kirchhoff index is proportional to the biharmonic distance [76], we can deduce that the gradient of the total  $k$ -harmonic distance is proportional to the  $(k + 1)$ -harmonic distance by a similar proof of Lemma 3.8.

While the strategies for selecting edges in the greedy process differ between Algorithm 1 and Algorithm 2, both approaches yield relatively effective solutions in the experimental evaluations presented in Section 5. This indicates that using the gradient instead of the marginal decrease is a feasible method. This method is very common and performs well in our problem. In the next section, based on Algorithm DETERGRAD, we design a nearly linear time algorithm to solve Problem 1.

---

#### Algorithm 2: DETERGRAD( $G, k$ )

---

**Input** : Graph  $G = (V, E)$ ; an integer  $k$

**Output** : An edge set  $T \subseteq Q$  of size  $k$

- 1 Compute  $L^\ddagger, L^{2\ddagger}, L^{3\ddagger}$
  - 2  $T = \emptyset, Q = (V \times V) \setminus E$
  - 3 **for**  $i = 1$  **to**  $k$  **do**
  - 4     Compute  $c(e)$  for each  $e \in Q$
  - 5     Select  $e_i$  s.t.  $e_i \leftarrow \arg \max_{e \in Q} c(e)$
  - 6      $T \leftarrow T \cup \{e_i\}, G \leftarrow G(V, E \cup \{e_i\}), Q \leftarrow Q \setminus \{e_i\}$
  - 7     Update  $L^\ddagger$  by (1),  $L^{2\ddagger}$  by (2), and  $L^{3\ddagger}$  by (4)
  - 8 **return**  $T$
- 

## 4 Fast Approximation Algorithm

Both Algorithm 1 and Algorithm DETERGRAD struggle with high time complexity, making them computationally prohibitive for large-scale networks. This challenge arises from several key factors. First, calculating  $c(e)$  requires inverting the Laplacian matrix, which has a time complexity of  $\Theta(n^3)$ , presenting a significant computational burden. Second, each iteration involves examining all pairs of nodes to identify an edge to add and requires querying  $|Q|$  gradients, where  $n^2 - m - k \leq |Q| \leq n^2 - m$ . This leads to a computational bottleneck. Finally, even with the use of the Sherman-Morrison formula to update  $L^\ddagger, L^{2\ddagger}$ , and  $L^{3\ddagger}$ , the time complexity per iteration remains  $O(n^2)$ . Our primary objective is to optimize three aspects for improved efficiency. We begin by addressing the highest time cost, which is our first challenge. To reduce the high computational cost associated with matrix inversion, we employ the projection technique and the Laplacian solver to estimate  $c(e)$ . This approach also eliminates the need to update  $L^\ddagger, L^{2\ddagger}$ , and  $L^{3\ddagger}$ , effectively addressing the third challenge simultaneously. For the second challenge, we introduce a pruning strategy based on geometric principles to approximate the convex hull, which helps to reduce the size of the candidate edge set. By integrating these methods, we propose an approximation algorithm, outlined in Algorithm 3. This algorithm achieves an  $\epsilon$ -approximation of  $c(e)$  in each of the  $k$  iterations, enabling approximate solutions with nearly linear time complexity.

#### 4.1 Projection Technique and Laplacian Solver

We begin by reformulating  $\mathbf{b}_e^\top \mathbf{L}^{3\ddagger} \mathbf{b}_e$  in terms of the  $\ell_2$ -norm.

$$\begin{aligned} \mathbf{b}_e^\top \mathbf{L}^{3\ddagger} \mathbf{b}_e &= (\mathbf{L}^\ddagger \mathbf{b}_e)^\top \mathbf{L}^\ddagger \mathbf{L}^\ddagger \mathbf{b}_e = (\mathbf{L}^\ddagger \mathbf{b}_e)^\top \mathbf{L}^\ddagger \mathbf{L} \mathbf{L}^\ddagger \mathbf{L}^\ddagger \mathbf{b}_e \\ &= (\mathbf{L}^\ddagger \mathbf{b}_e)^\top \mathbf{L}^\ddagger \mathbf{B}^\top \mathbf{B} \mathbf{L}^\ddagger \mathbf{L}^\ddagger \mathbf{b}_e = \|\mathbf{B} \mathbf{L}^{2\ddagger} (\mathbf{e}_u - \mathbf{e}_v)\|^2. \end{aligned}$$

In this way, computing  $c(e)$  reduces to computing  $\|\mathbf{B} \mathbf{L}^{2\ddagger} (\mathbf{e}_u - \mathbf{e}_v)\|^2$  in  $\mathbb{R}^m$ . However, calculating this exact  $\ell_2$ -norm is computationally intensive because the dimension  $m$  of the vectors  $\mathbf{B} \mathbf{L}^{2\ddagger} \mathbf{e}_i$  (where  $i = 1, 2, \dots, n$ ) is high, and it also requires matrix inversion. To alleviate this issue and reduce the dimensionality of the vectors, we employ the Johnson-Lindenstrauss lemma for dimensionality reduction.

LEMMA 4.1 ([1, 29]). *Given fixed vectors  $\mathbf{v}_1, \mathbf{v}_2, \dots, \mathbf{v}_n \in \mathbb{R}^d$  and  $\beta > 0$ , let  $\mathbf{Q}_{t \times d}$  be a random matrix, where each entry is either  $1/\sqrt{t}$  or  $-1/\sqrt{t}$ , with probability of  $1/2$ , and  $t \geq 24 \log(n)/\beta^2$ . Then, with probability at least  $1 - 1/n$ , the following holds for all pairs  $i, j \leq n$ :*

$$(1 - \beta) \|\mathbf{v}_i - \mathbf{v}_j\|_2^2 \leq \|\mathbf{Q} \mathbf{v}_i - \mathbf{Q} \mathbf{v}_j\|_2^2 \leq (1 + \beta) \|\mathbf{v}_i - \mathbf{v}_j\|_2^2.$$

Let  $\mathbf{Q} \in \mathbb{R}^{t \times m}$  be a random matrix with entries  $\pm 1/\sqrt{t}$ , where  $t = \lceil 24 \log(n)/\beta^2 \rceil$ . By Lemma 4.1, we have the approximation:

$$\|\mathbf{Q} \mathbf{B} \mathbf{L}^{2\ddagger} (\mathbf{e}_u - \mathbf{e}_v)\|^2 \approx_\beta \|\mathbf{B} \mathbf{L}^{2\ddagger} (\mathbf{e}_u - \mathbf{e}_v)\|^2 \quad (5)$$

for every pair  $(u, v)$  with probability at least  $1 - 1/n$ .

We have projected a set of  $n$   $m$ -dimensional vectors onto a low  $t$ -dimensional subspace spanned by the columns of the matrix  $\mathbf{Q}$ . However, the high computational cost of  $\Omega(n^3)$  associated with matrix inversion still exists. To circumvent this expensive operation, we utilize a fast SDD linear system solver to solve the corresponding linear equations.

LEMMA 4.2 ([13, 63]). *Let  $\mathbf{X} \in \mathbb{R}^{n \times n}$  be a positive semi-definite matrix with  $m$  nonzero entries, and  $\mathbf{b} \in \mathbb{R}^n$  a vector. For any error parameter  $\delta > 0$ , there exists a solver, denoted by  $\mathbf{a} = \text{SOLVE}(\mathbf{X}, \mathbf{b}, \delta)$ , which returns a vector  $\mathbf{a} \in \mathbb{R}^n$  satisfying*

$$\|\mathbf{a} - \mathbf{X}^{-1} \mathbf{b}\|_X \leq \delta \|\mathbf{X}^{-1} \mathbf{b}\|_X$$

with probability at least  $1 - 1/n$ . The expected runtime of this solver is  $\tilde{O}(m)$ , where  $\tilde{O}(\cdot)$  suppresses  $\text{poly}(\log(n))$  factors.

To approximate  $\|\mathbf{B} \mathbf{L}^{2\ddagger} (\mathbf{e}_u - \mathbf{e}_v)\|^2$ , we apply the solver as follows. For any small  $\beta > 0$ , we choose an appropriate  $\delta$  to ensure the approximation error remains within  $\beta$  with probability at least  $1 - 1/n$ . Let  $\mathbf{Z} = \mathbf{Q} \mathbf{B} \mathbf{L}^{2\ddagger}$ . We solve the system of equations  $\mathbf{L}^2 \mathbf{z}_i = \mathbf{y}_i$ , with the constraint  $\mathbf{1}^\top \mathbf{z}_i = 0$ , for  $i = 1, \dots, t$ , where  $\mathbf{z}_i^\top$  and  $\mathbf{y}_i^\top$  represent the  $i$ -th rows of  $\mathbf{Z}$  and  $\mathbf{Q} \mathbf{B}$ , respectively. By using the solver  $\text{SOLVE}(\mathbf{L}, \mathbf{y}_i, \delta)$  twice, and carefully selecting  $\delta$ , we achieve a reliable approximation of  $\mathbf{z}_i$ . Before proving this, we first introduce some lemmas (all missing proofs are provided in Appendix A).

LEMMA 4.3. *Given a Laplacian matrix  $\mathbf{L}$  and a vector  $\mathbf{z}$  orthogonal to  $\mathbf{1}$ , we have*

$$\|\mathbf{L}^\ddagger \mathbf{z}\|_L \leq 2n^4 \|\mathbf{z}\|_L. \quad (6)$$

**Proof.**  $\|\mathbf{L}^\ddagger \mathbf{z}\|_L = \sqrt{\mathbf{z}^\top \mathbf{L}^\ddagger \mathbf{z}} \leq \sqrt{2n^4} \|\mathbf{z}\|_L$ , and  $\|\mathbf{z}\|_L = \sqrt{\mathbf{z}^\top \mathbf{L} \mathbf{z}} \geq \frac{1}{\sqrt{2n^4}} \|\mathbf{z}\|$ , which further suggest that  $\|\mathbf{L}^\ddagger \mathbf{z}\|_L \leq 2n^4 \|\mathbf{z}\|_L$ .  $\square$

LEMMA 4.4. *Given two vector sequences  $\mathbf{z}^{(1)}, \mathbf{z}^{(2)}$  and  $\tilde{\mathbf{z}}^{(1)}, \tilde{\mathbf{z}}^{(2)}$  such that*

$$\mathbf{z}^{(1)} = \mathbf{L}^\ddagger \mathbf{y}, \quad \mathbf{z}^{(2)} = \mathbf{L}^\ddagger \mathbf{z}^{(1)},$$

and

$$\tilde{\mathbf{z}}^{(1)} = \text{SOLVE}(\mathbf{L}, \mathbf{y}, \delta), \quad \tilde{\mathbf{z}}^{(2)} = \text{SOLVE}(\mathbf{L}, \tilde{\mathbf{z}}^{(1)}, \delta),$$

we have the following error bound:

$$\|\tilde{\mathbf{z}}^{(2)} - \mathbf{z}^{(2)}\|_L \leq \delta' \|\mathbf{L}^\ddagger \mathbf{y}\|_L, \quad (7)$$

where  $\delta' = 2n^4 (\delta^2 + 2\delta)$ .

**Proof.** First, according to Lemma 4.2, we have

$$\|\tilde{\mathbf{z}}^{(1)} - \mathbf{L}^\ddagger \mathbf{y}\|_L \leq \delta \|\mathbf{L}^\ddagger \mathbf{y}\|_L, \quad (8)$$

$$\|\tilde{\mathbf{z}}^{(2)} - \mathbf{L}^\ddagger \tilde{\mathbf{z}}^{(1)}\|_L \leq \delta \|\mathbf{L}^\ddagger \tilde{\mathbf{z}}^{(1)}\|_L. \quad (9)$$

Since  $\|\cdot\|_L$  is a norm, (8) can be recast as

$$(1 - \delta) \|\mathbf{L}^\ddagger \mathbf{y}\|_L \leq \|\tilde{\mathbf{z}}^{(1)}\|_L \leq (1 + \delta) \|\mathbf{L}^\ddagger \mathbf{y}\|_L. \quad (10)$$

Then, we apply the triangle inequality on the left-hand side of (7):

$$\begin{aligned} \|\tilde{\mathbf{z}}^{(2)} - \mathbf{z}^{(2)}\|_L &\leq \|\tilde{\mathbf{z}}^{(2)} - \mathbf{L}^\ddagger \tilde{\mathbf{z}}^{(1)}\|_L + \|\mathbf{L}^\ddagger \tilde{\mathbf{z}}^{(1)} - \mathbf{L}^\ddagger \mathbf{z}^{(1)}\|_L \\ &\leq \delta \|\mathbf{L}^\ddagger \tilde{\mathbf{z}}^{(1)}\|_L + 2n^4 \|\tilde{\mathbf{z}}^{(1)} - \mathbf{z}^{(1)}\|_L \\ &\leq \delta (2n^4) \|\tilde{\mathbf{z}}^{(1)}\|_L + 2n^4 \delta \|\mathbf{L}^\ddagger \mathbf{y}\|_L \\ &\leq \delta (2n^4) (1 + \delta) \|\mathbf{L}^\ddagger \mathbf{y}\|_L + 2n^4 \delta \|\mathbf{L}^\ddagger \mathbf{y}\|_L \\ &\leq 2n^4 (\delta^2 + 2\delta) \|\mathbf{L}^\ddagger \mathbf{y}\|_L, \end{aligned}$$

where the second inequality is due to (6) and (8), the third inequality is due to (6) and the fourth inequality is due to (10).  $\square$

We then show the constructed  $\|\tilde{\mathbf{Z}} (\mathbf{e}_u - \mathbf{e}_v)\|^2$  is a reliable approximation of  $\|\mathbf{B} \mathbf{L}^{2\ddagger} (\mathbf{e}_u - \mathbf{e}_v)\|^2$  as stated in the following lemma.

LEMMA 4.5. *Given a  $t \times n$  matrix  $\mathbf{Z}$ , for any  $0 \leq \beta \leq 1/3$ , suppose that for any pair of nodes  $u, v \in V$ :*

$$(1 - \beta) \|\mathbf{B} \mathbf{L}^{2\ddagger} (\mathbf{e}_u - \mathbf{e}_v)\|^2 \leq \|\mathbf{Z} (\mathbf{e}_u - \mathbf{e}_v)\|^2 \leq (1 + \beta) \|\mathbf{B} \mathbf{L}^{2\ddagger} (\mathbf{e}_u - \mathbf{e}_v)\|^2.$$

Let  $\mathbf{z}_i^\top$  be the  $i$ -th row of  $\mathbf{Z}$ , and  $\tilde{\mathbf{z}}_i$  be an approximation of  $\mathbf{z}_i$ , satisfying

$$\|\mathbf{z}_i - \tilde{\mathbf{z}}_i\|_L \leq \delta' \|\mathbf{L}^\ddagger \mathbf{y}_i\|_L, \quad (11)$$

where

$$\delta' \leq \frac{\beta}{3n^2} \sqrt{\frac{2(1 - \beta)}{(1 + \beta)(n - 1)}}. \quad (12)$$

Then, for any node pair  $u, v \in V$ , the following relation holds

$$\|\tilde{\mathbf{Z}} (\mathbf{e}_u - \mathbf{e}_v)\|^2 \approx_{\frac{2}{3}\beta} \|\mathbf{B} \mathbf{L}^{2\ddagger} (\mathbf{e}_u - \mathbf{e}_v)\|^2. \quad (13)$$

To ensure Lemma 4.4 holds, we should carefully select  $\delta$  for the Laplacian solver. By substituting  $\delta' = 2n^4 (\delta^2 + 2\delta)$  from Lemma 4.4, we obtain the inequality  $\delta' = 2n^4 (\delta^2 + 2\delta) \leq \frac{\beta}{3n^2} \sqrt{\frac{2(1 - \beta)}{(1 + \beta)(n - 1)}}$ . This allows us to refine  $\delta$  as  $\delta \leq \left( \frac{\beta}{6n^6} \sqrt{\frac{2(1 - \beta)}{(n - 1)(1 + \beta)}} + 1 \right)^{1/2} - 1$ .

By setting  $\delta$  accordingly, we can have the approximation in Lemma 4.5. Although Lemma 4.2 ensures that we can estimate  $c(e)$  in  $\tilde{O}(m/\beta^2)$  time, evaluating  $c(e)$  for all edges in the candidate edge set  $\mathcal{Q}$  remains computationally demanding. To address this, we introduce a pruning technique to reduce the size of the candidate edge set.

## 4.2 Pruning Technique

In this subsection, we utilize a pruning technique based on the convex hull of a set of points [55]. This approach allows us to reduce the candidate edge set  $Q$  to a smaller subset  $P$  with  $P \subset Q$  and  $|P| \ll |Q|$ . This reduction improves the efficiency of our algorithm and provides approximate solutions for the optimization problem.

Based on (13), estimating  $c(e)$  can be reduced to calculating distances between  $O(n^2)$  pairs of points  $\tilde{Z}e_i$  in  $\mathbb{R}^t$ , where  $i = 1, 2, \dots, n$ . We denote a set  $P = \{p_1, p_2, \dots, p_n\}$ , where each  $p_i = \tilde{Z}e_i$ . To find the maximum gradient of  $c(e)$ , we need to identify the farthest pair of points among  $P$ . As distances between interior points are usually smaller than those involving boundary points, we concentrate on identifying the boundary points, which can be efficiently determined using the concept of the convex hull.

**DEFINITION 4.6** ([55]). *Given a set of  $n$  points  $P = \{p_1, p_2, \dots, p_n\}$  in  $\mathbb{R}^t$ , the convex hull of  $P$  is the minimal convex polytope that contains all the points in  $P$ . The boundary of this convex hull is denoted by  $C(P)$ , and the subset of points in  $P$  that lie on this boundary is denoted by  $\hat{P}$ .*

Below, we explain how to efficiently identify the convex hull of a set of points. For  $P = \{p_1, p_2, \dots, p_n\} \subset \mathbb{R}^t$ , the time complexity of finding the convex hull is  $O(n^{t/2})$  [11, 16], which is impractical, even when  $t = \lceil 24 \log(n)/\beta^2 \rceil$ . As a result, convex hull approximations are often utilized. Among the available methods, FASTHULL [4, 5, 30] offers the lowest time complexity while still providing an error guarantee. It outperforms other approaches, such as linear programming [57] and the semi-nonnegative matrix factorization method with a kernel trick [27]. We choose to use FASTHULL for approximating the convex hull due to its significantly lower time complexity [5]. The performance of the FASTHULL algorithm is captured in the following lemma. Let  $d(P)$  denote the diameter of the set  $P$ , defined as  $d(P) = \max_{p_i, p_j \in P} \|p_i - p_j\|_2$ . This represents the maximum distance between all pairs of points  $p_i$  and  $p_j$  and satisfies the relationship  $d(P) = d(\hat{P})$ .

**LEMMA 4.7** ([5]). *For a set of points  $P = \{p_1, p_2, \dots, p_n\} \subset \mathbb{R}^t$ , and a parameter  $\mu \in (0, 1)$ , the algorithm FASTHULL( $P, \mu$ ) generates an  $l$ -node subset  $\hat{P}$  of  $\hat{P}$ . The algorithm has a time complexity of  $O(nl(t + \mu^{-2}))$  and ensures that the Euclidean distance for any  $p \in \hat{P}$  to  $C(\hat{P})$  does not exceed  $\mu d(P)$ .*

We can obtain an approximate point set  $\hat{P} \subseteq \hat{P}$ , the boundary of convex hull  $C(P)$  by applying FASTHULL. It is easy to derive that  $d(\hat{P}) \geq (1 - 2\mu)d(P)$ . Since  $(1 - 2\mu)^2 \geq 1 - 4\mu$ , we have  $(1 - 4\mu)d(P)^2 \leq d(\hat{P})^2$ . Thus,

$$d(\hat{P})^2 \approx_{4\mu} d(P)^2. \quad (14)$$

According to Lemma 4.7 and (14), FASTHULL can efficiently approximate the convex hull for  $P$ . When  $t = \lceil 24 \log(n)/\beta^2 \rceil$ , the time complexity of FASTHULL is  $O(nl \log(n)\beta^{-2})$ . This approximation greatly reduces computation time, as we only need to query  $l$  times, and finding the furthest point pairs from the set  $\hat{P}$  now only needs  $O(l^2 \log(n)\beta^{-2})$ . Based on the above results, we now propose a fast algorithm, APPROXFAST, as detailed in Algorithm 3. The approximate ratio for each iteration is given by the following theorem.

---

### Algorithm 3: APPROXFAST( $G, \epsilon, k$ )

---

**Input** : Graph  $G = (V, E)$ ; a parameter  $\epsilon$ ; an integer  $k$   
**Output** : An edge set  $T \subseteq Q$  of size  $k$

- 1  $\mu = \epsilon/8, \beta = \frac{3}{14}\epsilon, \delta = \left( \frac{\beta}{6n^6} \sqrt{\frac{2(1-\beta)}{(n-1)(1+\beta)}} + 1 \right)^{1/2} - 1$
- 2  $T = \emptyset, L \leftarrow$  the Laplacian matrix of graph  $G$
- 3  $t = \lceil 24 \log(n)/\beta^2 \rceil$
- 4 Generate random Gaussian matrices  $Q \in \mathbb{R}^{t \times m}$
- 5 **for**  $i = 1$  **to**  $t$  **do**
- 6      $y_i^\top$  = the  $i$ -th row of  $QB$
- 7 **for**  $i = 1$  **to**  $k$  **do**
- 8     **for**  $j = 1$  **to**  $t$  **do**
- 9          $\tilde{z}_j^{(1)} = \text{SOLVE}(L, y_j, \delta)$
- 10          $\tilde{z}_j^{(2)} = \text{SOLVE}(L, \tilde{z}_j^{(1)}, \delta)$
- 11          $\tilde{z}_j = \tilde{z}_j^{(2)}$
- 12      $P = \{p_1, p_2, \dots, p_n\}$  with each point being  $\tilde{Z}_{:,1}, \tilde{Z}_{:,2}, \dots, \tilde{Z}_{:,n}$
- 13      $\hat{P} = \text{FASTHULL}(P, \mu)$
- 14      $(x, y) \leftarrow \arg \max_{u, v \in \hat{P}} \|\tilde{Z}_{:,u} - \tilde{Z}_{:,v}\|_2^2$
- 15      $T \leftarrow T \cup \{(x, y)\}, G \leftarrow G(V, E \cup \{(x, y)\})$
- 16     Update  $L$
- 17 **return**  $T$

---

**THEOREM 4.8.** *The gradient of the edge selected at each iteration is an  $\epsilon$ -approximation of the maximum gradient of the objective function.*

**Proof.** By Lemma 4.5, we have  $d(P)^2 \approx_{\frac{2}{3}\beta} \max_{u, v \in V} \|\mathbf{BL}^{2t}(\mathbf{e}_u - \mathbf{e}_v)\|^2$ . Combining this result with (14), it follows that  $d(\hat{P})^2 \approx_{\frac{2}{3}\beta + 4\mu} \max_{u, v \in V} \|\mathbf{BL}^{2t}(\mathbf{e}_u - \mathbf{e}_v)\|^2$ . Setting  $\beta = \frac{3}{14}\epsilon$  and  $\mu = \epsilon/8$ , we obtain  $d(\hat{P})^2 \approx_{\epsilon} \max_{e \in Q} c(e)$ , which implies that the gradient of the edge selected in each iteration provides an  $\epsilon$ -approximation of the maximum gradient of the objective function.  $\square$

The time complexity of Algorithm 3 is summarized in Theorem 4.9.

**THEOREM 4.9.** *Given a positive integer  $k$  and an error parameter  $\epsilon \in (0, 1)$ , the runtime of Algorithm 3 is in  $\tilde{O}(k(nl + m)/\epsilon^2)$ .*

The components, Laplacian solver and FASTHULL, of APPROXFAST play a mutually complementary role in the algorithm. Removing either part would significantly increase the time complexity, making it difficult to scale the algorithm to large networks. If only the Laplacian solver is used, the complexity of each iteration becomes  $O(n^2)$ ; if only FastHull is used, the complexity of each iteration becomes  $O(n^3)$ . So we did not conduct ablation studies in the subsequent experimental section.

## 5 Experiments

### 5.1 Experimental Setup

**Datasets.** We use 10 real-life networks from the Network Repository [56], SNAP [37] and KONECT [34]. Our experiments focus on the largest connected component (LCC) of these networks.

**Environment and Implementation.** All our experiments are conducted on a Linux server with a 2.10 GHz CPU and 128 GB of memory, with a single thread. We set  $\epsilon = 0.4$ . All the proposed algorithms are implemented in *Julia*, where the Laplace Solver is used from [36].

**Total Biharmonic Distance Computation.** For small graphs, we are able to compute the exact total biharmonic distance via computing  $L^\dagger$ . For medium and large networks, it is difficult to obtain the exact total biharmonic distance. So we do not perform an analysis of the actual approximation error. Instead, we compare the values of the total biharmonic distance returned by different algorithms—smaller values indicate smaller approximation errors. To efficiently compute the total biharmonic distance, we utilize Hutchinson’s Monte-Carlo method [28] and the Laplacian solver [13, 63] to approximate the total biharmonic distance with a provable guarantee, adhering to the methodology in [59].

**Edge Addition Strategies.** The set of  $k$  edges is selected by different strategies: OPTIMAL, RANDOM, ACGREEDY, DETERDIFF, DETERGRAD, and APPROXFAST. OPTIMAL selects the  $k$  edges that minimize  $B(G)$  via brute-force search. As we are the first to solve Problem 1, and no existing methods are available for direct comparison, we include several heuristic baselines. RANDOM selects  $k$  edges uniformly at random. ACGREEDY selects  $k$  edges that yield the greatest increase in algebraic connectivity [24], defined as the second smallest eigenvalue of  $L$ . This method is based on the Fiedler vector, which is computed efficiently via the Lanczos algorithm [17]. We choose this method as a baseline because  $B(G)$  is primarily influenced by the small eigenvalues of  $L$ , as shown in Definition 2.2. In subsequent figures, we use  $B(G)/n$  instead of  $B(G)$ .

Details including dataset statistics, and parameter sensitivity analysis are provided in Appendix A.3.

## 5.2 Effectiveness Comparison

We begin by evaluating the effectiveness of our algorithms by comparing them with OPTIMUM, RANDOM and ACGREEDY. To this end, we conduct experiments on four small networks: Tribes (16 nodes, 58 edges), Karate (34 nodes, 78 edges), Dolphins (62 nodes, 159 edges), and Moreno (64 nodes, 243 edges). Since these networks are small, we are able to obtain the optimal solution through exhaustive search. For each network, we select  $k = 1, 2, \dots, 5$  edges. Figure 2 illustrates how  $B(G)/n$  changes as  $k$  increases for each algorithm.

The following observations can be made. First, the values returned by three greedy algorithms are almost identical to OPTIMUM, with the four curves overlapping, indicating that DETERDIFF significantly outperforms its theoretical guarantee. DETERGRAD and APPROXFAST demonstrate effective performance in practice. Second, our proposed algorithms all perform better than RANDOM and ACGREEDY. To further demonstrate the effectiveness of our algorithms, we compare their performance with RANDOM and ACGREEDY on four moderately larger real-world networks, each with fewer than 10,000 nodes. These networks are large enough to make OPTIMUM impractical. For each network, Figure 3 shows the performance of each algorithm as  $k$  increases from 1 to 10. All of our proposed algorithms perform significantly better than ACGREEDY. Notably, DETERGRAD achieves results that are comparable to the standard greedy algorithm DETERDIFF, suggesting that selecting the edge

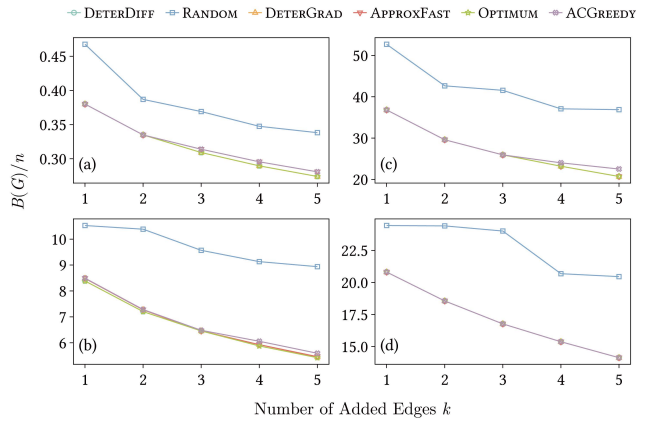


**Figure 2:**  $B(G)/n$  returned by six algorithms on four small networks: Tribes (a), Karate (b), Dolphins (c), and Moreno (d).

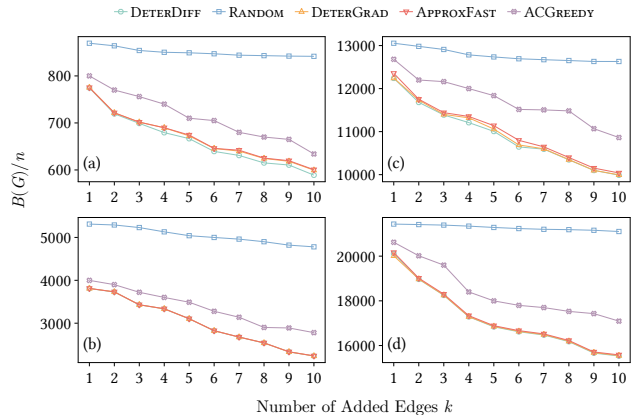


**Figure 3:**  $B(G)/n$  returned by five algorithms on four networks: Hamster (a), Facebook (b), Grqc (c), Hephth (d).

with the largest gradient is a highly effective strategy for Problem 1. Additionally, our fast approximation algorithm, APPROXFAST, yields similar results, further demonstrating its effectiveness.

## 5.3 Efficiency Comparison

Although our three greedy algorithms perform remarkably well in terms of effectiveness, we will demonstrate that APPROXFAST is significantly faster than DETERDIFF, DETERGRAD and ACGREEDY. To illustrate this, we compare the efficiency of these algorithms. Figure 4 presents the running time of these algorithms across various networks. For each network, we select  $k = 50$  edges. Notably, for both Facebook and Hephth networks, consisting of 4,039 and 8,638 nodes respectively, DETERGRAD and DETERDIFF take over 30 hours to select  $k = 50$  edges, making them impractical for networks larger than 10,000 nodes. Due to the extreme slowness of DETERGRAD and DETERDIFF, the curves of ACGREEDY and APPROXFAST appear to overlap for Facebook and Hephth. However, ACGREEDY is in fact

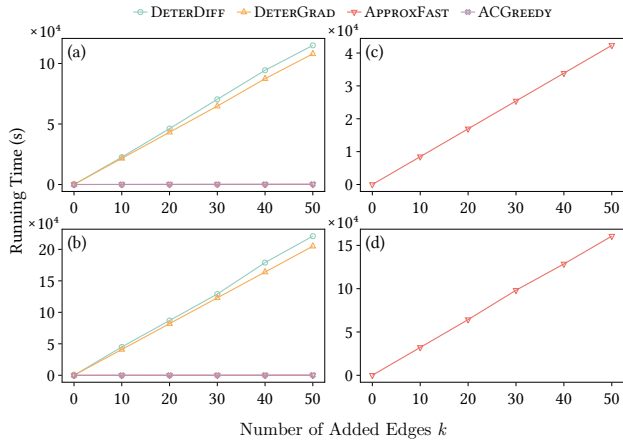


**Figure 4: Running time of different algorithms for  $k = 10, 20, \dots, 50$  on four networks: Facebook (a), Hepth (b), YoutubeSnap (c), and Livejournal (d).**

much slower than APPROXFAST. For  $k = 50$ , ACGREEDY takes 295 seconds on Facebook and 332 seconds on Hepth, while APPROXFAST completes in only 118 and 110 seconds, respectively. On the larger Douban network with 154,908 nodes, ACGREEDY takes over 10 hours for  $k = 50$ , whereas APPROXFAST finishes within 1 hour. This makes ACGREEDY unsuitable for networks with over 150,000 nodes. As a result, DETERDIFF, DETERGRAD, and ACGREEDY are omitted from Figure 4 for the YoutubeSnap and LiveJournal networks (Figures 4(c) and (d)), which have over 1 million nodes, as they could not complete within a reasonable time frame. In stark contrast, APPROXFAST shows remarkable efficiency, completing in just 2 minutes on both the Facebook and Hepth networks with  $k = 50$  edges. For YoutubeSnap, which has more than 1 million nodes and 2 million edges, APPROXFAST requires only 11 hours, and for the largest network, with over 4 million nodes and 27 million edges, APPROXFAST completes in 44 hours, both with  $k = 50$ . These results underscore the scalability and practicality of APPROXFAST.

Finally, we point out that since the optimal edge selection strategy depends on the optimization objective, and thus a specific edge selection strategy is required for a specific problem. Taking the minimization of the leading eigenvalue of a non-backtracking matrix as an example, if the edges are selected based on the reduction of the spectral radius of the adjacency matrix and the non-backtracking matrix, the resulting edge sets are very different [80]. Therefore, edge selection strategies are problem-dependent. ACGREEDY is specially designed to maximize algebraic connectivity. From our experiments, ACGREEDY performs significantly worse than our customized methods and fails to identify a more effective edge set.

## 6 Related Work

**Resistance Distance Computation.** Various algorithms have been developed for estimating resistance distances in large graphs [26, 41, 51, 75]. Early methods used random projection [62], while subsequent approaches improved efficiency through random walk

sampling and random spanning tree formulations [51]. More recent work introduced Monte Carlo techniques for faster random walk-based estimations [75] and landmark-based sampling methods [41, 42]. Despite extensive studies on resistance distance, its variants, such as biharmonic distance, remain less understood.

**Biharmonic Distance Computation.** Originally introduced by Lipman et al. [43], biharmonic distance captures global structural information and is more effective than resistance distance in network influence mining and graph embedding [9, 33, 76]. Several efficient algorithms for biharmonic distance computation have been proposed [44, 78, 79], but no methods have been developed to minimize total biharmonic distance through edge addition.

**Optimization via Edge Addition.** Edge addition has been studied for optimizing various objectives [14, 66, 74], such as increasing the number of spanning trees [38], reducing random walk hitting times [3], improving centrality measures [15, 40, 46, 59], and minimizing total shortest path distances [48]. Other objectives, which are more closely related to network connectivity and robustness, include reducing the network diameter [2, 23], bolstering algebraic connectivity [24], decreasing the Kirchhoff index [25, 32, 52], and increasing robustness [10]. We are the first to propose our problem. None of the existing approaches can be directly translated to the problem of minimizing total biharmonic distance through edge addition. Furthermore, existing approaches may face challenges when applied to large-scale networks. Our work addresses this gap by introducing novel algorithms specifically designed for this challenging optimization problem.

## 7 Conclusion

In this paper, we studied the problem of minimizing the total biharmonic distance in a network through link recommendation. We first demonstrated the monotonicity of the total biharmonic distance, showing that adding new edges to the graph decreases the total biharmonic distance. Based on this property, we formulated a combinatorial optimization problem with broad applicability, including network robustness maximization. The problem is combinatorially complex. We established that while the objective function of the problem is monotone, it is not supermodular. To tackle the problem, we employed greedy heuristics. The first algorithm, DETERDIFF, has a provable bound of approximation factor and cubic time complexity. The second algorithm, DETERGRAD, uses the gradient rather than the marginal decrease, showing selecting the edge with the largest gradient is an effective strategy. We then leveraged the projection technique, the Laplacian solver, and the convex hull approximation to develop an algorithm with nearly linear time complexity and an error guarantee. Finally, we performed experiments on ten real networks, showing that DETERDIFF, DETERGRAD, and APPROXFAST exhibit comparable effectiveness, with APPROXFAST being the most efficient. APPROXFAST demonstrates scalability in large graphs containing over 4 million nodes. Future work includes extending our algorithm for other network optimization problems.

## 8 Acknowledgments

The work was supported by the National Natural Science Foundation of China (Nos. 62372112 and 61872093).

## References

- [1] Dimitris Achlioptas. 2001. Database-friendly random projections. In *Proceedings of the Twentieth ACM SIGMOD-SIGACT-SIGART Symposium on Principles of Database Systems*. ACM, 274–281.
- [2] Florian Adriaens and Aristides Gionis. 2022. Diameter minimization by short-cutting with degree constraints. In *2022 IEEE International Conference on Data Mining*. IEEE, 843–848.
- [3] Florian Adriaens, Honglian Wang, and Aristides Gionis. 2023. Minimizing hitting time between disparate groups with shortcut edges. In *Proceedings of the 29th ACM SIGKDD Conference on Knowledge Discovery and Data Mining*, 1–10.
- [4] Pranjal Awasthi, Bahman Kalantari, and Yikai Zhang. 2018. Robust vertex enumeration for convex hulls in high dimensions. In *International Conference on Artificial Intelligence and Statistics*. PMLR, 1387–1396.
- [5] Pranjal Awasthi, Bahman Kalantari, and Yikai Zhang. 2020. Robust vertex enumeration for convex hulls in high dimensions. *Annals of Operations Research* 295, 1 (2020), 37–73.
- [6] Bassam Bamieh, Mihailo R Jovanovic, Partha Mitra, and Stacy Patterson. 2012. Coherence in large-scale networks: Dimension-dependent limitations of local feedback. *IEEE Trans. Automat. Control* 57, 9 (2012), 2235–2249.
- [7] Andrew An Bian, Joachim M Buhmann, Andreas Krause, and Sebastian Tschitschek. 2017. Guarantees for greedy maximization of non-submodular functions with applications. In *Proceedings of the 34th International Conference on Machine Learning*. JMLR, 498–507.
- [8] Mitchell Black, Lucy Lin, Amir Nayyeri, and Weng-Keen Wong. 2024. Biharmonic distance of graphs and its higher-order variants: Theoretical properties with applications to centrality and clustering. In *International Conference on Machine Learning*. PMLR, 4077–4102.
- [9] Mitchell Black, Zhengchao Wan, Amir Nayyeri, and Yusu Wang. 2023. Understanding oversquashing in GNNs through the lens of effective resistance. In *International Conference on Machine Learning*. PMLR, 2528–2547.
- [10] Hau Chan and Leman Akoglu. 2016. Optimizing network robustness by edge rewiring: a general framework. *Data Mining and Knowledge Discovery* 30 (2016), 1395–1425.
- [11] Bernard Chazelle. 1993. An optimal convex hull algorithm in any fixed dimension. *Discrete & Computational Geometry* 10, 4 (1993), 377–409.
- [12] Fan RK Chung. 1997. *Spectral Graph Theory*. Vol. 92. American Mathematical Soc.
- [13] Michael B Cohen, Rasmus Kyng, Gary L Miller, Jakub W Pachocki, Richard Peng, Anup B Rao, and Shen Chen Xu. 2014. Solving SDD linear systems in nearly  $m \log^{1/2} n$  time. In *Proceedings of the Forty-Sixth Annual ACM Symposium on Theory of Computing*. ACM, 343–352.
- [14] Pierluigi Crescenzi, Gianlorenzo D’angelo, Lorenzo Severini, and Yllka Velaj. 2016. Greedily improving our own closeness centrality in a network. *ACM Transactions on Knowledge Discovery from Data* 11, 1 (2016), 9.
- [15] Gianlorenzo D’Angelo, Martin Olsen, and Lorenzo Severini. 2019. Coverage centrality maximization in undirected networks. In *Proceedings of the 33rd AAAI Conference on Artificial Intelligence*, Vol. 33. 501–508.
- [16] Mark de Berg, Otfried Cheong, Marc van Kreveld, and Mark Overmars. 2008. *Computational Geometry: Algorithms and Applications*. Springer.
- [17] James W Demmel. 1997. *Applied Numerical Linear Algebra*. SIAM.
- [18] Florian Dörfler and Francesco Bullo. 2013. Kron reduction of graphs with applications to electrical networks. *IEEE Transactions on Circuits and Systems—I. Regular Papers* 60, 1 (2013), 150–163.
- [19] Florian Dörfler, John W Simpson-Porco, and Francesco Bullo. 2018. Electrical networks and algebraic graph theory: Models, properties, and applications. *Proc. IEEE* 106, 5 (2018), 977–1005.
- [20] Zhou Fan, Cheng Mao, Yihong Wu, and Jiaming Xu. 2020. Spectral graph matching and regularized quadratic relaxations: Algorithm and theory. In *International Conference on Machine Learning*. PMLR, 2985–2995.
- [21] Katherine Fitch and Naomi Ehrich Leonard. 2015. Joint centrality distinguishes optimal leaders in noisy networks. *IEEE Transactions on Control of Network Systems* 3, 4 (2015), 366–378.
- [22] Francois Fouss, Alain Pirotte, J-M Renders, and Marco Saerens. 2007. Random-walk computation of similarities between nodes of a graph with application to collaborative recommendation. *IEEE Transactions on Knowledge and Data Engineering* 19, 3 (2007), 355–369.
- [23] Fabrizio Frati, Serge Gaspers, Joachim Gudmundsson, and Luke Mathieson. 2015. Augmenting graphs to minimize the diameter. *Algorithmica* 72, 4 (2015), 995–1010.
- [24] Arpita Ghosh and Stephen Boyd. 2006. Growing well-connected graphs. In *Proceedings of the 45th IEEE Conference on Decision and Control*. IEEE, 6605–6611.
- [25] Arpita Ghosh, Stephen Boyd, and Amin Saberi. 2008. Minimizing effective resistance of a graph. *SIAM Rev.* 50, 1 (2008), 37–66.
- [26] Takanori Hayashi, Takuya Akiba, and Yuichi Yoshida. 2016. Efficient algorithms for spanning tree centrality. In *Proceedings of the 25th International Joint Conference on Artificial Intelligence*. 3733–3739.
- [27] Chengqiang Huang, Yulei Wu, Geyong Min, and Yiming Ying. 2018. Kernelized convex hull approximation and its applications in data description tasks. In *2018 International Joint Conference on Neural Networks*. IEEE, 1–8.
- [28] MF Hutchinson. 1989. A stochastic estimator of the trace of the influence matrix for Laplacian smoothing splines. *Communications in Statistics-Simulation and Computation* 18, 3 (1989), 1059–1076.
- [29] William B Johnson and Joram Lindenstrauss. 1984. Extensions of Lipschitz mappings into a Hilbert space. *Contemp. Math.* 26 (1984), 189–206.
- [30] Bahman Kalantari. 2015. A characterization theorem and an algorithm for a convex hull problem. *Annals of Operations Research* 226 (2015), 301–349.
- [31] Douglas J Klein and Milan Randić. 1993. Resistance distance. *Journal of Mathematical Chemistry* 12, 1 (1993), 81–95.
- [32] Robert E Kooij and Massimo A Achterberg. 2023. Minimizing the effective graph resistance by adding links is NP-hard. *Operations Research Letters* 51, 6 (2023), 601–604.
- [33] Devin Kreuzer, Dominique Beaini, Will Hamilton, Vincent Létourneau, and Prudencio Tossou. 2021. Rethinking graph transformers with spectral attention. *Advances in Neural Information Processing Systems* 34, 21618–21629.
- [34] Jérôme Kunegis. 2013. Konect: The koblenz network collection. In *Proceedings of the 22nd International Conference on World Wide Web*. ACM, 1343–1350.
- [35] Jérôme Kunegis and Stephan Schmidt. 2007. Collaborative filtering using electrical resistance network models. In *Industrial Conference on Data Mining*. Springer, 269–282.
- [36] Rasmus Kyng and Sushant Sachdeva. 2016. Approximate Gaussian elimination for Laplacians-fast, sparse, and simple. In *Proceedings of the IEEE 57th Annual Symposium on Foundations of Computer Science*. IEEE, 573–582.
- [37] Jure Leskovec and Rok Sosić. 2016. Snap: A general-purpose network analysis and graph-mining library. *ACM Transactions on Intelligent Systems and Technology* 8, 1 (2016), 1–20.
- [38] Huan Li, Stacy Patterson, Yuhao Yi, and Zhongzhi Zhang. 2019. Maximizing the number of spanning trees in a connected graph. *IEEE Transactions on Information Theory* 66, 2 (2019), 1248–1260.
- [39] Huan Li and Zhongzhi Zhang. 2018. Kirchhoff index as a measure of edge centrality in weighted networks: Nearly linear time algorithms. In *Proceedings of the 29th Annual ACM-SIAM Symposium on Discrete Algorithms*. 2377–2396.
- [40] Wentao Li, Min Gao, Fan Wu, Wenge Rong, Junhao Wen, and Lu Qin. 2021. Manipulating black-box networks for centrality promotion. In *2021 IEEE 37th International Conference on Data Engineering*. IEEE, 73–84.
- [41] Meihao Liao, Rong-Hua Li, Qiangqiang Dai, Hongyang Chen, Hongchao Qin, and Guoren Wang. 2023. Efficient resistance distance computation: The power of landmark-based approaches. *Proceedings of the ACM on Management of Data* 1, 1 (2023), 1–27.
- [42] Meihao Liao, Junjie Zhou, Rong-Hua Li, Qiangqiang Dai, Hongyang Chen, and Guoren Wang. 2024. Efficient and provable effective resistance computation on large graphs: An index-based approach. *Proceedings of the ACM on Management of Data* 2, 3 (2024), 1–27.
- [43] Y. Lipman, R.M. Rustamov, and T.A. Funkhouser. 2010. Biharmonic distance. *ACM Transactions on Graphics* 29 (2010), 1–11.
- [44] Changan Liu, Ahad N Zehmakan, and Zhongzhi Zhang. 2024. Fast query of biharmonic distance in networks. In *Proceedings of the 30th ACM SIGKDD Conference on Knowledge Discovery and Data Mining*. 1887–1897.
- [45] Zenan Lu, Xiaotian Zhou, Ahad N Zehmakan, and Zhongzhi Zhang. 2024. Resistance eccentricity in graphs: Distribution, computation and optimization. In *2024 IEEE 40th International Conference on Data Engineering*. IEEE, 4113–4126.
- [46] Sourav Medya, Arlei Silva, Ambuj Singh, Prithwish Basu, and Ananthram Swami. 2018. Group centrality maximization via network design. In *Proceedings of the 2018 SIAM International Conference on Data Mining*. SIAM, 126–134.
- [47] Carl D Meyer, Jr. 1973. Generalized inversion of modified matrices. *SIAM J. Appl. Math.* 24, 3 (1973), 315–323.
- [48] Adam Meyerson and Brian Tagiku. 2009. Minimizing average shortest path distances via shortcut edge addition. In *International Workshop on Approximation Algorithms for Combinatorial Optimization*. Springer, 272–285.
- [49] George L Nemhauser, Laurence A Wolsey, and Marshall L Fisher. 1978. An analysis of approximations for maximizing submodular set functions-I. *Mathematical Programming* 14, 1 (1978), 265–294.
- [50] Mark Newman. 2018. *Networks*. Oxford University Press.
- [51] Pan Peng, Daniel Lopatta, Yuichi Yoshida, and Gramoz Goranci. 2021. Local algorithms for estimating effective resistance. In *Proceedings of the 27th ACM SIGKDD Conference on Knowledge Discovery & Data Mining*. 1329–1338.
- [52] Maria Predari, Robert Kooij, and Henning Meyerhenke. 2022. Faster greedy optimization of resistance-based graph robustness. In *2022 IEEE/ACM International Conference on Advances in Social Networks Analysis and Mining*. IEEE, 1–8.
- [53] Yi Qi, Zhongzhi Zhang, Yuhao Yi, and Huan Li. 2018. Consensus in self-similar hierarchical graphs and Sierpiński graphs: Convergence speed, delay robustness, and coherence. *IEEE Transactions on Cybernetics* 49, 2 (2018), 592–603.
- [54] Jiezhong Qiu, Laxman Dhulipala, Jie Tang, Richard Peng, and Chi Wang. 2021. Lightne: A lightweight graph processing system for network embedding. In

- Proceedings of the 2021 International Conference on Management of Data*. 2281–2289.
- [55] R Tyrrell Rockafellar. 1970. *Convex Analysis*. Vol. 18. Princeton University Press.
- [56] Ryan Rossi and Nesreen Ahmed. 2015. The network data repository with interactive graph analytics and visualization. In *Proceedings of the AAAI Conference on Artificial Intelligence*, Vol. 29.
- [57] Antonio Ruano, Hamid Reza Khosravani, and Pedro M Ferreira. 2015. A randomized approximation convex hull algorithm for high dimensions. *IFAC-PapersOnLine* 48, 10 (2015), 123–128.
- [58] Purnamrita Sarkar, Andrew W Moore, and Amit Prakash. 2008. Fast incremental proximity search in large graphs. In *Proceedings of the 25th International Conference on Machine Learning*. 896–903.
- [59] Liren Shan, Yuhao Yi, and Zhongzhi Zhang. 2018. Improving information centrality of a node in complex networks by adding edges. *27th International Joint Conference on Artificial Intelligence*, 3535–3541.
- [60] Jianbo Shi and Jitendra Malik. 2000. Normalized cuts and image segmentation. *IEEE Transactions on Pattern Analysis and Machine Intelligence* 22, 8 (2000), 888–905.
- [61] Milad Siami and Nader Motee. 2017. Growing linear dynamical networks endowed by spectral systemic performance measures. *IEEE Trans. Automat. Control* 63, 7 (2017), 2091–2106.
- [62] Daniel A Spielman and Nikhil Srivastava. 2008. Graph sparsification by effective resistances. In *Proceedings of the fortieth Annual ACM Symposium on Theory of Computing*. 563–568.
- [63] Daniel A Spielman and Shang-Hua Teng. 2014. Nearly linear time algorithms for preconditioning and solving symmetric, diagonally dominant linear systems. *SIAM J. Matrix Anal. Appl.* 35, 3 (2014), 835–885.
- [64] Kumar Sricharan and Kamalika Das. 2014. Localizing anomalous changes in time-evolving graphs. In *Proceedings of the 2014 ACM SIGMOD International Conference on Management of Data*. 1347–1358.
- [65] J Michael Steele. 2004. *The Cauchy-Schwarz Master Class: An Introduction to the Art of Mathematical Inequalities*. Cambridge University Press.
- [66] Manuel Then, Moritz Kaufmann, Fernando Chirigati, Tuan-Anh Hoang-Vu, Kien Pham, Alfons Kemper, Thomas Neumann, and Huy T Vo. 2014. The more the merrier: Efficient multi-source graph traversal. *Proceedings of the VLDB Endowment* 8, 4 (2014), 449–460.
- [67] Krishnaiyan Thulasiraman, Mamta Yadav, and Kshirasagar Naik. 2018. Network science meets circuit theory: Resistance distance, Kirchhoff index, and Foster’s theorems with generalizations and unification. *IEEE Transactions on Circuits and Systems I: Regular Papers* 66, 3 (2018), 1090–1103.
- [68] Ali Tizghadam and Alberto Leon-Garcia. 2010. Autonomic traffic engineering for network robustness. *IEEE Journal on Selected Areas in Communications* 28, 1 (2010).
- [69] Melvyn Tylo, Tommaso Coletta, and Ph Jacquod. 2018. Robustness of synchrony in complex networks and generalized Kirchhoff indices. *Physical Review Letters* 120, 8 (2018), 084101.
- [70] Melvyn Tylo, Laurent Pagnier, and Philippe Jacquod. 2019. The key player problem in complex oscillator networks and electric power grids: Resistance centralities identify local vulnerabilities. *Science Advances* 5, 11 (2019), eaaw8359.
- [71] Saurabh Verma and Zhi-Li Zhang. 2017. Hunt for the unique, stable, sparse and fast feature learning on graphs. *Advances in Neural Information Processing Systems* 30 (2017).
- [72] Yulong Wei, Rong-hua Li, and Weihua Yang. 2021. Biharmonic distance of graphs. *arXiv preprint arXiv:2110.02656* (2021).
- [73] Wanyue Xu, Bin Wu, Zuobai Zhang, Zhongzhi Zhang, Haibin Kan, and Guanrong Chen. 2022. Coherence scaling of noisy second-order scale-free consensus networks. *IEEE Transactions on Cybernetics* 52, 7 (2022), 5923–5934.
- [74] Wanyue Xu and Zhongzhi Zhang. 2023. Minimizing polarization in noisy leader-follower opinion dynamics. In *Proceedings of the 32nd ACM International Conference on Information and Knowledge Management*. 2856–2865.
- [75] Renchi Yang and Jing Tang. 2023. Efficient estimation of pairwise effective resistance. *Proceedings of the ACM on Management of Data* 1, 1 (2023), 1–27.
- [76] Yuhao Yi, Liren Shan, Huan Li, and Zhongzhi Zhang. 2018. Biharmonic distance related centrality for edges in weighted networks. In *Proceedings of the 27th International Joint Conference on Artificial Intelligence*. 3620–3626.
- [77] Yuhao Yi, Bingjia Yang, Zhongzhi Zhang, and Stacy Patterson. 2018. Biharmonic distance and performance of second-order consensus networks with stochastic disturbances. In *2018 Annual American Control Conference*. IEEE, 4943–4950.
- [78] Yuhao Yi, Bingjia Yang, Zuobai Zhang, Zhongzhi Zhang, and Stacy Patterson. 2021. Biharmonic distance-based performance metric for second-order noisy consensus networks. *IEEE Transactions on Information Theory* 68, 2 (2021), 1220–1236.
- [79] Zuobai Zhang, Wanyue Xu, Yuhao Yi, and Zhongzhi Zhang. 2020. Fast approximation of coherence for second-order noisy consensus networks. *IEEE Transactions on Cybernetics* 52, 1 (2020), 677–686.
- [80] Zuobai Zhang, Zhongzhi Zhang, and Guanrong Chen. 2021. Minimizing spectral radius of non-backtracking matrix by edge removal. In *Proceedings of the 30th*

*ACM International Conference on Information & Knowledge Management*. 2657–2667.

- [81] Xiaojin Zhu, Zoubin Ghahramani, and John D. Lafferty. 2003. Semi-supervised learning using gaussian fields and harmonic functions. In *Proceedings of the 20th International Conference on Machine Learning*. 912–919.

## A APPENDIX

In this section, we give proofs of Lemma 4.5 and Theorem 4.9. We also include additional experimental details.

### A.1 Proof of Lemma 4.5

**Proof.** In order to prove the lemma, it suffices to show that for any arbitrary pair of nodes  $u$  and  $v$ ,

$$\begin{aligned} & \left| \|Z(\mathbf{e}_u - \mathbf{e}_v)\|^2 - \|\tilde{Z}(\mathbf{e}_u - \mathbf{e}_v)\|^2 \right| \\ &= \left| \|Z(\mathbf{e}_u - \mathbf{e}_v)\| - \|\tilde{Z}(\mathbf{e}_u - \mathbf{e}_v)\| \right| \times \left| \|Z(\mathbf{e}_u - \mathbf{e}_v)\| + \|\tilde{Z}(\mathbf{e}_u - \mathbf{e}_v)\| \right| \\ &\leq \left( \frac{2\beta}{3} + \frac{\beta^2}{9} \right) \|Z(\mathbf{e}_u - \mathbf{e}_v)\|^2, \end{aligned} \quad (15)$$

which is satisfied if

$$\left| \|Z(\mathbf{e}_u - \mathbf{e}_v)\| - \|\tilde{Z}(\mathbf{e}_u - \mathbf{e}_v)\| \right| \leq \frac{\beta}{3} \|Z(\mathbf{e}_u - \mathbf{e}_v)\|. \quad (16)$$

The following arguments can account for this. First, if

$$\|Z(\mathbf{e}_u - \mathbf{e}_v)\|^2 - \|\tilde{Z}(\mathbf{e}_u - \mathbf{e}_v)\|^2 \leq \left( \frac{2\beta}{3} + \frac{\beta^2}{9} \right) \|Z(\mathbf{e}_u - \mathbf{e}_v)\|^2,$$

then it follows that

$$(1 - \beta)\|Z(\mathbf{e}_u - \mathbf{e}_v)\|^2 \leq \|\tilde{Z}(\mathbf{e}_u - \mathbf{e}_v)\|^2 \leq (1 + \beta)\|Z(\mathbf{e}_u - \mathbf{e}_v)\|^2.$$

Given the hypothesis

$$(1 - \beta)\|BL^{2^\dagger}(\mathbf{e}_u - \mathbf{e}_v)\|^2 \leq \|Z(\mathbf{e}_u - \mathbf{e}_v)\|^2 \leq (1 + \beta)\|BL^{2^\dagger}(\mathbf{e}_u - \mathbf{e}_v)\|^2,$$

we have

$$(1 - \beta)^2\|BL^{2^\dagger}(\mathbf{e}_u - \mathbf{e}_v)\|^2 \leq \|\tilde{Z}(\mathbf{e}_u - \mathbf{e}_v)\|^2 \leq (1 + \beta)^2\|BL^{2^\dagger}(\mathbf{e}_u - \mathbf{e}_v)\|^2,$$

which directly leads to (13).

In turn, if (16) holds true, then

$$\|\tilde{Z}(\mathbf{e}_u - \mathbf{e}_v)\| \leq \left( 1 + \frac{3}{\beta} \right) \|Z(\mathbf{e}_u - \mathbf{e}_v)\|.$$

Thus, we obtain the bound

$$\left| \|Z(\mathbf{e}_u - \mathbf{e}_v)\| + \|\tilde{Z}(\mathbf{e}_u - \mathbf{e}_v)\| \right| \leq \left( 2 + \frac{\beta}{3} \right) \|Z(\mathbf{e}_u - \mathbf{e}_v)\|,$$

which directly leads to (15).

We next prove that (16) holds true. Let  $P$  denote a simple path connecting  $u$  and  $v$ . Applying the triangle inequality along  $P$ , we obtain

$$\begin{aligned} & \left| \|Z(\mathbf{e}_u - \mathbf{e}_v)\| - \|\tilde{Z}(\mathbf{e}_u - \mathbf{e}_v)\| \right| \leq \|(Z - \tilde{Z})(\mathbf{e}_u - \mathbf{e}_v)\| \\ &\leq \sum_{a \sim b \in P} \|(Z - \tilde{Z})(\mathbf{e}_a - \mathbf{e}_b)\| \\ &\leq \left( n \sum_{a \sim b \in P} \|(Z - \tilde{Z})(\mathbf{e}_a - \mathbf{e}_b)\|^2 \right)^{1/2} \\ &\leq n^{1/2} \left( \sum_{a \sim b \in E} \|(Z - \tilde{Z})(\mathbf{e}_a - \mathbf{e}_b)\|^2 \right)^{1/2} \\ &= n^{1/2} \|(Z - \tilde{Z})\mathbf{B}^\top\|_F, \end{aligned}$$

where the third inequality is derived by Cauchy-Schwarz Inequality.

We now transform the above obtained Frobenius norm  $n^{1/2}\|(Z - \tilde{Z})B^\top\|_F$  into the  $L$ -norm as

$$\begin{aligned} n^{1/2}\|(Z - \tilde{Z})B^\top\|_F &= n^{1/2}\sqrt{\text{Tr}\left((Z - \tilde{Z})B^\top B(Z - \tilde{Z})^\top\right)} \\ &= n^{1/2}\sqrt{\text{Tr}\left((Z - \tilde{Z})L(Z - \tilde{Z})^\top\right)} \\ &= n^{1/2}\sqrt{\sum_{i=1}^m (z_i - \tilde{z}_i)^\top L(z_i - \tilde{z}_i)} \\ &\leq n^{1/2}\delta' \|QL^\dagger B^\top\|_F, \end{aligned}$$

where the inequality is obtained according to (11) and  $\delta'$  is given by (12). We continue to simplify  $n^{1/2}\delta' \|QL^\dagger B^\top\|_F$  as

$$\begin{aligned} n^{1/2}\delta' \|QL^\dagger B^\top\|_F &= n^{1/2}\delta' \left(\sum_{a \sim b \in E} \|QL^\dagger(\mathbf{e}_a - \mathbf{e}_b)\|^2\right)^{1/2} \\ &\leq n^{1/2}\delta' \left((1 + \beta) \sum_{a \sim b \in E} R_{a,b}\right)^{1/2} \\ &= n^{1/2}\delta' ((1 + \beta)(n - 1))^{1/2}. \end{aligned}$$

On the other hand, we provide a lower bound of  $\|Z(\mathbf{e}_u - \mathbf{e}_v)\|$  as

$$\|Z(\mathbf{e}_u - \mathbf{e}_v)\|^2 \geq (1 - \beta)(\mathbf{e}_u - \mathbf{e}_v)^\top L^{3\ddagger}(\mathbf{e}_u - \mathbf{e}_v).$$

The eigenvalues of the Laplacian matrix  $L$  of  $G$  are at most  $n$ , so the non-zero eigenvalues of  $L^\ddagger$  are at least  $\frac{1}{n}$  and the non-zero eigenvalues of  $L^{3\ddagger}$  are at least  $\frac{1}{n^3}$ . Moreover, the vector  $\mathbf{e}_u - \mathbf{e}_v$  is orthogonal to  $\ker L$ , since  $\ker L$  is spanned by the all-ones vector. By the Courant-Fischer theorem, which states that for a symmetric matrix  $A$  with minimal non-zero eigenvalue  $\lambda_{\min}$ , and for any non-zero vector  $\mathbf{x} \perp \ker A$ , we have  $\lambda_{\min} \leq \frac{\mathbf{x}^\top A \mathbf{x}}{\mathbf{x}^\top \mathbf{x}}$ . Thus, we obtain

$$(\mathbf{e}_u - \mathbf{e}_v)^\top L^{3\ddagger}(\mathbf{e}_u - \mathbf{e}_v) \geq \frac{2}{n^3}.$$

Therefore,

$$\|Z(\mathbf{e}_u - \mathbf{e}_v)\|^2 \geq (1 - \beta) \frac{2}{n^3}.$$

Combining the above-obtained results, it follows that

$$\begin{aligned} &\frac{\|Z(\mathbf{e}_u - \mathbf{e}_v)\| - \|\tilde{Z}(\mathbf{e}_u - \mathbf{e}_v)\|}{\|Z(\mathbf{e}_u - \mathbf{e}_v)\|} \\ &\leq \delta' n^2 ((1 + \beta)(n - 1))^{1/2} \left(\frac{1}{2(1 - \beta)}\right)^{1/2} \leq \frac{\beta}{3}. \end{aligned}$$

This completes the proof.  $\square$

## A.2 Proof of Theorem 4.9

**Proof.** We begin by analyzing the time complexity of the algorithm. First, a random matrix  $Q$  is generated, which takes  $O(m \log n / \epsilon^2)$  time (Line 4). Next, we compute  $QB$ , which requires  $2m \times 24 \log n \epsilon^{-2} = \tilde{O}(m \epsilon^{-2})$  time, as  $B$  contains  $2m$  entries (Lines 5-6). The algorithm proceeds through  $k$  iterative rounds (Lines 7-16), with each round selecting a single edge. During each iteration, the Laplacian solver is applied  $2t$  times, resulting in a total cost of  $2 \times 24 \log n \epsilon^{-2} \times m = \tilde{O}(m \epsilon^{-2})$ . Consequently, the points  $\{p_1, p_2, \dots, p_n\}$  are computed in  $\tilde{O}(m \epsilon^{-2})$  time (Lines 8-12).

Subsequently, the convex hull of the point set  $P$  is computed using APPROXCONV, with a time complexity of  $O(n \log n \epsilon^{-2} t)$  (Line 13). The maximum distance between points on the convex hull

is then determined in  $O(t^2 \log n \epsilon^{-2})$  time (Line 14). Finally, the solution, the graph, and the Laplacian matrix are updated based on the identified results (Lines 15-16). Thus, the overall time complexity of the APPROXFAST algorithm is  $\tilde{O}(k(nl + m)/\epsilon^2)$ .  $\square$

## A.3 Experimental Details

**A.3.1 Datasets Used in Experiments.** Table 1 provides the details of each network.

**Table 1: Datasets used in experiments.**

| Type           | Networks    | $n$       | $m$        |
|----------------|-------------|-----------|------------|
| Small Network  | Tribes      | 16        | 58         |
|                | Karate      | 34        | 78         |
|                | Dolphins    | 62        | 159        |
|                | Moreno      | 64        | 243        |
| Medium Network | Hamster     | 2,000     | 16,097     |
|                | Facebook    | 4,039     | 88,234     |
|                | Grqc        | 4,158     | 13,422     |
| Large Network  | Hepth       | 8,638     | 24,806     |
|                | YoutubeSnap | 1,134,890 | 2,987,624  |
|                | Livejournal | 4,033,137 | 27,933,062 |

**A.3.2 Parameter Sensitivity Analysis.** We further examine the influence of varying error parameter  $\epsilon$  on the accuracy and efficiency of APPROXFAST. Specifically, we conduct a series of experiments across several real-world networks, adjusting  $\epsilon$  within the range of 0.2 to 0.5. According to the results in Table 2, the running time of APPROXFAST increases approximately in proportion to  $\epsilon^{-2}$ , which empirically supports its theoretical time complexity of  $\tilde{O}(k(nl + m)/\epsilon^2)$ . In addition, Table 2 reveals that the results returned by APPROXFAST remain similar as  $\epsilon$  changes.

**Table 2: The running time (seconds, s) and  $B(G)/n$  returned by APPROXFAST when  $k = 10$  on real-world networks.**

| Networks     | Running time (s) |                |                |                | $B(G)/n$       |                |                |                |
|--------------|------------------|----------------|----------------|----------------|----------------|----------------|----------------|----------------|
|              | $\epsilon=0.2$   | $\epsilon=0.3$ | $\epsilon=0.4$ | $\epsilon=0.5$ | $\epsilon=0.2$ | $\epsilon=0.3$ | $\epsilon=0.4$ | $\epsilon=0.5$ |
| Hamster      | 40               | 16             | 10             | 6              | 588            | 592            | 594            | 604            |
| Facebook     | 91               | 42             | 24             | 16             | 2178           | 2198           | 2215           | 2245           |
| Grqc         | 71               | 32             | 19             | 12             | 9900           | 9988           | 10011          | 10049          |
| Hepth        | 80               | 35             | 23             | 14             | 15452          | 15497          | 15532          | 15582          |
| Youtube Snap | 32863            | 14036          | 8465           | 5418           | 4470080        | 4471300        | 4472020        | 4473103        |